

# Symbol-by-Symbol Maximum Likelihood Detection for Cooperative Molecular Communication

Yuting Fang, *Student Member, IEEE*, Adam Noel, *Member, IEEE*, Nan Yang, *Member, IEEE*, Andrew W. Eckford, *Senior Member, IEEE*, and Rodney A. Kennedy, *Fellow, IEEE*

**Abstract**—In this paper, symbol-by-symbol maximum likelihood (ML) detection is proposed for a cooperative diffusion-based molecular communication (MC) system. In this system, a fusion center (FC) chooses the transmitter (TX) symbol that is more likely, given the likelihood of its observations from multiple receivers (RXs), where the TX sends a common information symbol to all RXs. The transmission of a sequence of binary symbols and the resultant intersymbol interference are considered in the cooperative MC system. We propose five ML detection variants according to different constraints on the knowledge at the FC. These five variants demonstrate trade-offs between their performance and the information available. The system error probabilities for three ML detector variants are derived, two of which are in closed form. Numerical and simulation results show that the ML detection variants provide lower bounds on the error performance of the simpler cooperative variants and demonstrate that these simpler cooperative variants have error performance comparable to ML detectors when the reporting from RXs to the FC is noisy.

**Index Terms**—Molecular communication, multi-receiver cooperation, symbol-by-symbol maximum likelihood detection, error performance.

## I. INTRODUCTION

Over the past decades, the incredible advancements in nanotechnology and biological science have enabled the miniaturisation and fabrication of nanomachines with simple computation, sensing, communication, and actuation capabilities. To expand the limited capabilities of a single nanomachine, the concept of nanonetworks has been envisioned to interconnect nanomachines to execute complex tasks in a collaborative and distributed manner. Despite the prevalence of radio transmission, electromagnetic waves are not always practical for interconnecting nanomachines. Specifically, radio-frequency transceivers cannot be easily integrated into nanomachines, due to component size, and would not have enough power to establish a bidirectional communication channel. Molecular communication (MC) has been heralded as one of the most promising paradigms to implement communication in bio-inspired nanonetworks, due to the potential benefits of bio-compatibility and low energy consumption; see [1]. In MC, the information transmission between devices is realized through the exchange of molecules; see [2].

Y. Fang, N. Yang, and R. A. Kennedy are with the Research School of Engineering, Australian National University, Canberra, ACT 2601, Australia (e-mail: {yuting.fang, nan.yang, rodney.kennedy}@anu.edu.au).

A. Noel is with the School of Electrical Engineering and Computer Science, University of Ottawa, Ottawa, ON K1N 6N5, Canada (e-mail: anoel2@uottawa.ca).

A. W. Eckford is with the Department of Electrical Engineering and Computer Science, York University, Toronto, ON M3J 1P3, Canada (e-mail: aeckford@yorku.ca)

The simplest molecular propagation mechanism is free diffusion, where the information-carrying molecules can propagate from the transmitter (TX) to the receiver (RX) via Brownian motion. One of the primary challenges posed by diffusion-based MC is that its reliability rapidly decreases when the TX-RX distance increases. A naturally-inspired approach, which also makes use of the envisioned collaboration between nanomachines, is allowing multiple RXs to share information for cooperative detection. Often, cells or organisms share common information to achieve a specific task, e.g., calcium ( $\text{Ca}^{2+}$ ) signaling; see [3]. In  $\text{Ca}^{2+}$  signaling,  $\text{Ca}^{2+}$ -insensitive channels detect  $\text{Ca}^{2+}$  mobilizing messengers and release  $\text{Ca}^{2+}$  to the cytosol. When gap junctions are formed between adjacent cells, the release of  $\text{Ca}^{2+}$  is also triggered in these cells. Then, the cells share  $\text{Ca}^{2+}$  ions to complete a specific task, such as muscle contraction; see [4].

The majority of existing MC studies have focused on the modeling of a single-RX MC system. Recent studies, e.g., [5]–[12], have expanded the single-RX MC system to a multi-RX MC system. Although these studies stand on their own merit, they did not establish the potential of *active cooperation* among multiple RXs to determine a TX’s intended symbol sequence in a multi-RX MC system. To address this gap, our work in [13]–[15] analyzed the error performance of a cooperative diffusion-based MC system where a fusion center (FC) device combines the binary decisions of distributed RXs to improve the detection of a TX’s symbols.

In other fields of communications, e.g., wireless communications, the maximum likelihood (ML) detector is commonly used to optimize detection performance; see [16, Ch. 5]. In the MC domain, the ML sequence detector has been considered for optimality in several studies. For example, [17] proposed a sequence detection variant based on a ML criterion to recover the transmitted information distorted by intersymbol interference (ISI) and noise. [18], [19] also considered variations to modify the Viterbi algorithm and reduce the computational complexity of optimal detection. However, the high complexity of sequence detection is a significant barrier to implement in the MC domain, even when applying simplified algorithms.

We note that the (suboptimal) symbol-by-symbol ML detector requires less computational complexity than the ML sequence detector. Motivated by this, [20], [21] considered symbol-by-symbol ML detection for MC with a single RX. Recently, [22]–[24] considered cooperative ML detection for MC. However, [22], [23] considered detection of an event and [24] considered detection of the presence of an undesired biological agent, i.e., [22]–[24] did not consider the detection of modulated information from a TX.

In this paper, we present symbol-by-symbol ML detection

for the cooperative diffusion-based MC system. The significance of this paper is that (i) our results provide lower bounds on the error performance that can be achieved by a practical cooperative MC system and (ii) demonstrate the good performance of more realizable cooperative variants considered in [13]–[15] relative to symbol-by-symbol ML variants, particularly when we impose reasonable constraints on the knowledge available at the FC. In this paper, we consider relatively simple RXs and keep the relatively high complexity associated with ML detection at the FC. This approach is because the RXs may be distributed as needed, for example throughout the body, whereas the FC could have a direct interface with the macroscopic world and easier access to computational resources.

In our proposed system, the transmission of each information symbol from the TX to the FC via the RXs is completed in two phases, as shown in Fig. 1. In the first phase, the TX sends a symbol that is observed by all RXs. In the second phase, the RXs send their detected information to the FC and the FC chooses the TX symbol that is more likely, given the (joint) likelihood of its observations from all of the individual RXs. We note that sequences of multiple symbols will be used to exchange the information to execute complex tasks (such as disease detection) and binary symbols are the easiest to transmit and detect. Thus, we consider the transmission of a sequence of binary symbols and account for the resultant ISI in the design and analysis of the cooperative MC system. The ISI at the RXs and the FC is due to the previous symbols transmitted by the TX and the RXs, respectively. To the best of the authors' knowledge, combined with our previous work in [25], this work is the *first* to apply symbol-by-symbol ML detection to a cooperative MC system with multiple communication phases.

For tractability, we assume that the system has a symmetric topology such that the distances between the TX and the RXs are identical and the distances between the RXs and the FC are also identical. This assumption could be relaxed in future work. We note that for some practical applications, such as health monitoring, we may be able to manually set the locations of the RXs and FC to ensure that the topology of the TX (e.g., monitored organism), the RXs (e.g., detectors), and the FC, is symmetric.

In this paper, we present a number of variants of symbol-by-symbol ML detectors, which are summarized in Table I. The variants are organized according to the knowledge at the FC, and enable us to demonstrate trade-offs in their performance versus the information available. First, we categorize the detectors according to their knowledge of the observations at the RX, i.e., perfect reporting detectors and noisy reporting detectors. Detectors with perfect knowledge of the RXs provide a lower bound on variants where the FC has to receive a noisy signal from each RX. The perfect variants are also more appropriate for non-diffusive reporting channels, such as the neurons considered in [26]. Second, we categorize the detectors that use noisy reporting according to how the RXs send information to the FC. These variants use either decode-and-forward (DF) relaying, where each RX makes a local decision that is propagated to the FC, or amplify-and-

forward (AF) relaying, where each RX amplifies the signal that it observes without making a local decision. Generally, AF does not perform as well as DF (see [27]), but is more suitable for devices with limited computational resources. We note that ML detection in the current symbol interval requires knowing the previously-transmitted symbols by the TX (and by all the RXs for DF). For convenience, we refer to the FC-estimated previous symbols as local history and the perfect knowledge of the previous symbols as genie-aided history.

Our major contributions are summarized as follows:

- 1) We present novel symbol-by-symbol ML detection designs for the cooperative MC system with all detector variants, i.e., F-ML, L-ML, SD-ML, MD-ML, and SA-ML. In our design, for practicality, the FC chooses the current symbol using its *local history*. The five variants reveal trade-offs among the performance, knowledge of previously-transmitted symbols, the types of molecule available, and computational complexity.
- 2) We derive analytical expressions for the system error probability for L-ML, SD-ML, and SA-ML using the *genie-aided history*. The assumption of genie-aided history leads to tractable error performance analysis. The analytical error probabilities for L-ML and SA-ML are given in closed form. We note that the error performance of F-ML and MD-ML is mathematically intractable.
- 3) Using simulation and numerical results, we demonstrate the FC's effectiveness in estimating the previously-transmitted symbols for all ML detector variants. We corroborate the accuracy of our analytical expressions for the system error probability using the genie-aided history. Importantly, we demonstrate that symbol-by-symbol ML detection can provide lower bounds on the error performance achieved by the simpler cooperative variants considered in [13]–[15]. We further demonstrate the good performance of these simpler and more realizable cooperative variants relative to symbol-by-symbol ML variants when the reporting from RXs to the FC is noisy.

We note that in contrast to our preliminary work in [25], which only presents ML detection design of F-ML, L-ML, and SD-ML, and derives the system error probability for L-ML, this paper presents two additional detector variants, i.e., MD-ML and SA-ML, and derives the system error probability for SD-ML and SA-ML. Moreover, many of the extensive analytical discussions and comprehensive comparisons of numerical and simulation results provided in this paper are not included in [25].

*Notations:* We use the following notations in this paper:  $\Pr(\cdot)$  denotes probability.  $\lfloor x \rfloor$  denotes the greatest integer that is less than or equal to  $x$ ,  $\lceil x \rceil$  denotes the smallest integer that is greater than or equal to  $x$ , and  $\lfloor \cdot \rfloor$  denotes the nearest integer.  $\log(\cdot)$  is the natural logarithm,  $\text{erf}(\cdot)$  is the error function, and  $\exp(\cdot)$  is the exponential function.  $|\cdot|$  is the cardinality of a set.

TABLE I  
VARIANTS OF ML DETECTORS

ML Detection Variants	Acronym	Reporting Scenario
Full Knowledge ML Detection	F-ML	Perfect
Limited Knowledge ML Detection	L-ML	Perfect
DF with Multi-molecule-type and ML Detection at the FC	MD-ML	Noisy
DF with Single-molecule-type and ML Detection at the FC	SD-ML	Noisy
AF with Single-molecule-type and ML detection at the FC	SA-ML	Noisy

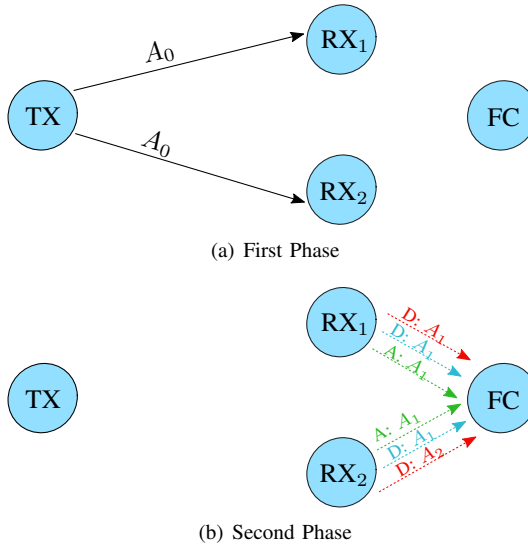


Fig. 1. An example of a cooperative MC system with  $K = 2$ . In (a), the transmission from the TX to the RXs is represented by black solid arrows. In (b), for the transmission from the RXs to the FC, we consider MD-ML, SD-ML, and SA-ML which are represented by red, blue, and green dashed arrows, respectively. In (b), “D” denotes the RXs making decisions and “A” denotes the RXs amplifying observations. We emphasize that the second stage shown in (b) only applies to noisy reporting.

## II. SYSTEM MODEL AND PRELIMINARIES

### A. System Model

We consider a cooperative MC system in a three-dimensional space based on [13]–[15], which consists of one TX, a “cluster” of  $K$  RXs, and an FC. An example of the cooperative MC system is illustrated in Fig. 1. For reliable reporting, we generally assume that the FC is relatively close to the cluster of RXs. We also assume that all RXs and the FC are passive spherical observers such that molecules can diffuse through them without reacting. Accordingly, we denote  $V_{\text{RX}_k}$  and  $r_{\text{RX}_k}$  as the volume and the radius of the  $k$ th RX,  $\text{RX}_k$ , respectively, where  $k \in \{1, 2, \dots, K\}$ . We also denote  $r_{\text{FC}}$  as the radius of the FC. We use the terms “sample” and “observation” interchangeably to refer to the number of molecules observed by a RX or the FC at some time  $t$ . We assume that the time between samples is sufficiently large and the distances between RXs are sufficiently large for all individual observations to be independent of each other. In this paper, the transmission interval time from the TX to the RXs is denoted by  $t_{\text{trans}}$  and the report interval time from the RXs to the FC is denoted by  $t_{\text{report}}$ . Thus, the symbol interval time from the TX to the FC is given by  $T = t_{\text{trans}} + t_{\text{report}}$ .

In the following, we present the timing schedule of the TX, the RXs, and the FC. At the beginning of the  $j$ th

symbol interval, i.e.,  $(j-1)T$ , the TX transmits  $W_{\text{TX}}[j]$ . The TX transmits  $W_{\text{TX}}[j]$  to the RXs over the diffusive channel via type  $A_0$  molecules which diffuse independently. The TX uses ON/OFF keying [28] to convey information, i.e., the TX releases  $S_0$  molecules of type  $A_0$  to convey information symbol “1” with probability  $\Pr(W_{\text{TX}}[j] = 1) = P_1$ , but no molecules to convey information symbol “0”. The TX then keeps silent until the start of the  $(j+1)$ th symbol interval. We denote  $L$  as the number of symbols transmitted by the TX. We define  $\mathbf{W}_{\text{TX}}^l = \{W_{\text{TX}}[1], \dots, W_{\text{TX}}[l]\}$  as an  $l$ -length subsequence of the symbols transmitted by the TX, where  $l \leq L$ . Throughout the paper,  $W$  is a single information symbol and  $\mathbf{W}$  is a vector of information symbols.

Each RX $_k$  observes type  $A_0$  molecules over the TX – RX $_k$  link and takes  $M_{\text{RX}}$  samples in each symbol interval at the same times<sup>1</sup>. The time of the  $m$ th sample by each RX in the  $j$ th symbol interval is given by  $t_{\text{RX}}(j, m) = (j-1)T + m\Delta t_{\text{RX}}$ , where  $\Delta t_{\text{RX}}$  is the time step between two successive samples by each RX,  $m \in \{1, 2, \dots, M_{\text{RX}}\}$ , and  $M_{\text{RX}}\Delta t_{\text{RX}} < t_{\text{trans}}$ . For noisy reporting variants, at the time  $(j-1)T + t_{\text{trans}}$ , each RX transmits molecules via a diffusion-based channel to the FC. The time of the  $\tilde{m}$ th sample by the FC in the  $j$ th symbol interval is given by  $t_{\text{FC}}(j, \tilde{m}) = (j-1)T + t_{\text{trans}} + \tilde{m}\Delta t_{\text{FC}}$ , where  $\Delta t_{\text{FC}}$  is the time step between two successive samples by the FC and  $\tilde{m} \in \{1, 2, \dots, M_{\text{FC}}\}$ .

We summarize the ML detection variants in Table I. The ML detection design for each variant is detailed in Section III. We denote  $\hat{W}_{\text{FC}}[j]$  as the FC’s decision on the  $j$ th symbol transmitted by the TX. We define  $\hat{\mathbf{W}}_{\text{FC}}^l = \{\hat{W}_{\text{FC}}[1], \dots, \hat{W}_{\text{FC}}[l]\}$  as an  $l$ -length subsequence of the FC’s decisions on the symbols transmitted by the TX.

### B. Preliminaries

In this subsection, we establish some fundamental preliminary results for a TX – RX $_k$  link and a RX $_k$  – FC link. These preliminary results are needed to evaluate the likelihoods in the ML detection variants in Section III.

1) TX – RX $_k$  Link: We first evaluate the probability  $P_{\text{ob}}^{(\text{TX}, \text{RX}_k)}(t)$  of observing a given type  $A_0$  molecule, emitted from the TX at  $t = 0$ , inside  $V_{\text{RX}_k}$  at time  $t$ . Assuming that the RXs are sufficiently far from the TX, we use [18, Eq. (13)] to write  $P_{\text{ob}}^{(\text{TX}, \text{RX}_k)}(t)$  as

$$P_{\text{ob}}^{(\text{TX}, \text{RX}_k)}(t) = \frac{V_{\text{RX}_k}}{(4\pi D_0 t)^{3/2}} \exp\left(-\frac{d_{\text{TX}}^2}{4D_0 t}\right), \quad (1)$$

<sup>1</sup>We note that various methods can be adopted to achieve time synchronization among nanomachines, e.g., [29], [30]. The assumption of perfect synchronization is widely adopted in existing MC studies, e.g., [11], [31], [32].

where  $D_0$  is the diffusion coefficient of type  $A_0$  molecules in  $\text{m}^2/\text{s}$  and  $d_{\text{TX}}$  is the distance between the TX and  $\text{RX}_k$  in m. We denote  $S_{\text{ob}}^{\text{RX}_k}(t)$  as the number of molecules observed within  $V_{\text{RX}_k}$  at time  $t$  due to  $\mathbf{W}_{\text{TX}}^{\lfloor \frac{t}{T} + 1 \rfloor}$ . As discussed in [18],  $S_{\text{ob}}^{\text{RX}_k}(t)$  can be accurately approximated by a Poisson random variable (RV) with the mean given by

$$\bar{S}_{\text{ob}}^{\text{RX}_k}(t) = \sum_{i=1}^{\lfloor \frac{t}{T} + 1 \rfloor} S_0 W_{\text{TX}}[i] P_{\text{ob}}^{(\text{TX}, \text{RX}_k)}(t - (i-1)T). \quad (2)$$

The sum of  $M_{\text{RX}}$  samples by  $\text{RX}_k$  in the  $j$ th symbol interval,  $S_{\text{ob}}^{\text{RX}_k}[j] = \sum_{m=1}^{M_{\text{RX}}} S_{\text{ob}}^{\text{RX}_k}(t_{\text{RX}}(j, m))$ , is also a Poisson RV. The mean of  $S_{\text{ob}}^{\text{RX}_k}[j]$  is given by

$$\bar{S}_{\text{ob}}^{\text{RX}_k}[j] = \sum_{i=1}^j S_0 W_{\text{TX}}[i] \sum_{m=1}^{M_{\text{RX}}} P_{\text{ob}}^{(\text{TX}, \text{RX}_k)}((j-i)T + m\Delta t_{\text{RX}}). \quad (3)$$

2)  $\text{RX}_k - \text{FC}$  Link: For MD-ML and SD-ML, each RX detects with a relatively simple *energy* detector. We denote  $\hat{W}_{\text{RX}_k}[j]$  as  $\text{RX}_k$ 's binary decision on the  $j$ th transmitted symbol. Based on the energy detector,  $\text{RX}_k$  makes decision  $\hat{W}_{\text{RX}_k}[j] = 1$  if  $s_j^{\text{RX}_k} \geq \xi_{\text{RX}_k}$ , otherwise  $\hat{W}_{\text{RX}_k}[j] = 0$ , where  $s_j^{\text{RX}_k}$  is the value of the realization of  $S_{\text{ob}}^{\text{RX}_k}[j]$  and  $\xi_{\text{RX}_k}$  is the constant detection threshold at  $\text{RX}_k$ , independent of  $\mathbf{W}_{\text{TX}}^{j-1}$ . We define  $\hat{\mathbf{W}}_{\text{RX}_k}^l = \{\hat{W}_{\text{RX}_k}[1], \dots, \hat{W}_{\text{RX}_k}[l]\}$  as an  $l$ -length subsequence of  $\text{RX}_k$ 's binary decisions. We denote  $P_{\text{ob},k}^{(\text{RX}_k, \text{FC})}(t)$  as the probability of observing a given  $A_k$  molecule, emitted from the center of  $\text{RX}_k$  at  $t = 0$ , inside  $V_{\text{FC}}$  at time  $t$ . Due to the relatively close proximity between the RXs and the FC, we find that (1) cannot be used to evaluate  $P_{\text{ob},k}^{(\text{RX}_k, \text{FC})}(t)$ . Thus, we resort to [32, Eq. (27)] to evaluate  $P_{\text{ob},k}^{(\text{RX}_k, \text{FC})}(t)$  as<sup>2</sup>

$$P_{\text{ob},k}^{(\text{RX}_k, \text{FC})}(t) = \frac{1}{2} [\text{erf}(\tau_1) + \text{erf}(\tau_2)] - \frac{\sqrt{D_k t}}{d_{\text{FC}_k} \sqrt{\pi}} [\exp(-\tau_1^2) - \exp(-\tau_2^2)], \quad (4)$$

where  $\tau_1 = \frac{r_{\text{FC}} + d_{\text{FC}_k}}{2\sqrt{D_k t}}$ ,  $\tau_2 = \frac{r_{\text{FC}} - d_{\text{FC}_k}}{2\sqrt{D_k t}}$ ,  $D_k$  is the diffusion coefficient of type  $A_k$  molecules in  $\text{m}^2/\text{s}$ , and  $d_{\text{FC}_k}$  is the distance between  $\text{RX}_k$  and the FC in m.

### III. ML DETECTION DESIGN

In this section, we present the design of *symbol-by-symbol* ML detection for the cooperative MC system. Throughout Section III, the FC uses the *local* history to choose the current symbol. We denote  $\hat{W}_{\text{FC}_k}[j]$  as the FC's estimated binary decision of  $\text{RX}_k$  on the  $j$ th transmitted symbol. We define  $\hat{\mathbf{W}}_{\text{FC}_k}^l = \{\hat{W}_{\text{FC}_k}[1], \dots, \hat{W}_{\text{FC}_k}[l]\}$  as the FC's estimate of the first  $l$  binary decisions by  $\text{RX}_k$ . In our symbol-by-symbol ML detection design, the FC evaluates the likelihood of the observations in the  $j$ th symbol interval based on its own local history, i.e.,  $\hat{\mathbf{W}}_{\text{FC}}^{j-1}$  (and  $\hat{\mathbf{W}}_{\text{FC}_k}^{j-1}$  for MD-ML and SD-ML). Using the local history at the FC, we formulate the general

<sup>2</sup>We note that (4) is accurate for any  $d_{\text{FC}_k} > 0$ , while (1) is accurate only when the RX is sufficiently far from the TX; see [32].

decision rule of ML detection on the  $j$ th symbol transmitted by the TX as

$$\hat{W}_{\text{FC}}[j] = \underset{W_{\text{TX}}[j] \in \{0, 1\}}{\text{argmax}} \mathcal{L}[j | W_{\text{TX}}[j], \hat{\mathbf{W}}_{\text{FC}}^{j-1}] \quad (5)$$

or

$$\hat{W}_{\text{FC}}[j] = \underset{W_{\text{TX}}[j] \in \{0, 1\}}{\text{argmax}} \mathcal{L}[j | W_{\text{TX}}[j], \hat{\mathbf{W}}_{\text{FC}}^{j-1}, \hat{\mathbf{W}}_{\text{FC}_k}^{j-1}], \quad (6)$$

where we define  $\mathcal{L}[j | \cdot] \triangleq \Pr(\text{FC's observations in } j\text{th interval} | \cdot)$ . We clarify that (5) applies to ML-F, ML-L, and SA-ML and (6) applies to SD-ML and MD-ML. For the sake of simplicity, we also define  $\mathcal{L}[j | W_{\text{TX}}[j], \hat{\mathbf{W}}_{\text{FC}}^{j-1}] \triangleq \mathcal{L}[j]$  for F-ML, L-ML, and SA-ML. We further define  $\mathcal{L}[j | W_{\text{TX}}[j], \hat{\mathbf{W}}_{\text{FC}}^{j-1}, \hat{\mathbf{W}}_{\text{FC}_k}^{j-1}] \triangleq \mathcal{L}[j]$  for MD-ML and SD-ML. In the remainder of this section, we present the detailed communication process and the evaluation of  $\mathcal{L}[j]$  for the ML detection variants in the perfect and noisy reporting scenarios.

#### A. Perfect Reporting

In the perfect reporting scenario, we only consider one-phase transmission of each information symbol from the TX to the RXs (see Fig. 1(a)), since the FC has perfect knowledge of the observations at all RXs. In this reporting scenario, we consider F-ML and L-ML.

1) *F-ML*: The FC separately assesses the likelihood of every sample by each RX and chooses the symbol  $\hat{W}_{\text{FC}}[j]$  that is more likely, given the joint likelihood of  $K M_{\text{RX}}$  *individual* observations at all RXs in the  $j$ th symbol interval. Recalling that all individual observations are independent of each other,  $\mathcal{L}[j]$  is given by

$$\mathcal{L}[j] = \prod_{k=1}^K \prod_{m=1}^{M_{\text{RX}}} \Pr\left(S_{\text{ob}}^{\text{RX}_k}(t_{\text{RX}}(j, m)) = s_{j,m}^{\text{RX}_k} | W_{\text{TX}}[j], \hat{\mathbf{W}}_{\text{FC}}^{j-1}\right), \quad (7)$$

where  $s_{j,m}^{\text{RX}_k}$  is the value of the realization of  $S_{\text{ob}}^{\text{RX}_k}(t_{\text{RX}}(j, m))$ .

2) *L-ML*: The FC adds each RX's  $M_{\text{RX}}$  observations in the  $j$ th symbol interval, i.e., the FC applies an equal weight to every observation at each RX. The FC chooses the symbol  $\hat{W}_{\text{FC}}[j]$  that is more likely, given the joint likelihood of  $K$  *sums* of  $s_j^{\text{RX}_k}$  in the  $j$ th symbol interval, where  $s_j^{\text{RX}_k} = \sum_{m=1}^{M_{\text{RX}}} s_{j,m}^{\text{RX}_k}$ . Recalling that the  $K$  RXs are independent,  $\mathcal{L}[j]$  is given by

$$\mathcal{L}[j] = \prod_{k=1}^K \Pr\left(S_{\text{ob}}^{\text{RX}_k}[j] = s_j^{\text{RX}_k} | W_{\text{TX}}[j], \hat{\mathbf{W}}_{\text{FC}}^{j-1}\right). \quad (8)$$

It is shown that (7) and (8) can be evaluated by the conditional probability mass function (PMF) of  $S_{\text{ob}}^{\text{RX}_k}(t)$  and  $S_{\text{ob}}^{\text{RX}_k}[j]$ . The conditional means of  $S_{\text{ob}}^{\text{RX}_k}(t)$  and  $S_{\text{ob}}^{\text{RX}_k}[j]$  given  $\hat{\mathbf{W}}_{\text{FC}}^{j-1}$  are obtained by replacing  $W_{\text{TX}}[i]$  with  $\hat{W}_{\text{FC}}[i]$  in (2) and (3), respectively, where  $i \in \{1, \dots, j-1\}$ .

### B. Noisy Reporting

In the noisy reporting scenario, the transmission of each information symbol from the TX to the FC via the RXs is completed in two phases (see Figs. 1(a) and 1(b)). The first phase of the noisy reporting scenario is analogous to the one-phase transmission of perfect reporting. For the second phase, we consider three different communication variants between the RXs and the FC over a diffusion channel, namely, MD-ML, SD-ML, and SA-ML. In the following, we describe the communication process of these variants and evaluate their corresponding  $\mathcal{L}[j]$ .

1) *MD-ML*:  $\text{RX}_k$  transmits type  $A_k$  molecules, which can be independently detected by the FC, to report  $\hat{W}_{\text{RX}_k}[j]$  to the FC. Similar to the TX, each RX uses ON/OFF keying to report its decision to the FC and the RX releases  $S_{\text{D}}$  molecules of type  $A_k$  to convey information symbol “1”. The FC receives type  $A_k$  molecules over the  $\text{RX}_k - \text{FC}$  link and takes  $M_{\text{FC}}$  samples of each of the  $K$  types of molecules transmitted by all RXs in every reporting interval. The FC adds  $M_{\text{FC}}$  observations for each  $\text{RX}_k - \text{FC}$  link in the  $j$ th symbol interval. We denote  $S_{\text{ob},k}^{\text{FC,D}}[j]$  as the total number of  $A_k$  molecules observed within  $V_{\text{FC}}$  in the  $j$ th symbol interval, due to both current and previous emissions of molecules by  $\text{RX}_k$ . We emphasize that the TX and  $\text{RX}_k$  use the same modulation method and that the  $\text{TX} - \text{RX}_k$  and  $\text{RX}_k - \text{FC}$  links are both diffusion-based. Therefore,  $S_{\text{ob},k}^{\text{FC,D}}[j]$  can also be accurately approximated by a Poisson RV. We denote  $\bar{S}_{\text{ob},k}^{\text{FC,D}}[j]$  as the mean of  $S_{\text{ob},k}^{\text{FC,D}}[j]$ . Values of realizations of  $S_{\text{ob},k}^{\text{FC,D}}[j]$  are labeled  $s_{j,k}^{\text{FC}}$ . We assume that the  $K$   $\text{RX}_k - \text{FC}$  links are independent, so the FC has  $K$  independent sums  $s_{j,k}^{\text{FC}}$  from the  $K$   $\text{RX}_k - \text{FC}$  links. The FC chooses the symbol  $\hat{W}_{\text{FC}}[j]$  that is more likely, given the joint likelihood of the  $K$  sums  $s_{j,k}^{\text{FC}}$  in the  $j$ th interval<sup>3</sup>. We obtain  $\mathcal{L}[j]$  by

$$\begin{aligned} \mathcal{L}[j] = \prod_{k=1}^K & \left[ \Pr \left( \hat{W}_{\text{RX}_k}[j] = 1 | W_{\text{TX}}[j], \hat{\mathbf{W}}_{\text{FC}}^{j-1} \right) \right. \\ & \times \Pr \left( S_{\text{ob},k}^{\text{FC,D}}[j] = s_{j,k}^{\text{FC}} | \hat{W}_{\text{RX}_k}[j] = 1, \hat{\mathbf{W}}_{\text{FC}_k}^{j-1} \right) \\ & + \Pr \left( \hat{W}_{\text{RX}_k}[j] = 0 | W_{\text{TX}}[j], \hat{\mathbf{W}}_{\text{FC}}^{j-1} \right) \\ & \left. \times \Pr \left( S_{\text{ob},k}^{\text{FC,D}}[j] = s_{j,k}^{\text{FC}} | \hat{W}_{\text{RX}_k}[j] = 0, \hat{\mathbf{W}}_{\text{FC}_k}^{j-1} \right) \right]. \quad (9) \end{aligned}$$

For the evaluation of the likelihood in all future intervals, i.e.,  $\mathcal{L}[j+1], \dots, \mathcal{L}[L]$ , the FC also chooses the symbol  $\hat{W}_{\text{FC}_k}[j]$  in the  $j$ th interval given the likelihood of the sum  $s_{j,k}^{\text{FC}}$  from the  $\text{RX}_k - \text{FC}$  link in the  $j$ th interval. By doing so,  $\hat{W}_{\text{FC}_k}[j]$  is obtained by

$$\hat{W}_{\text{FC}_k}[j] = \underset{\hat{W}_{\text{RX}_k}[j] \in \{0,1\}}{\operatorname{argmax}} \Pr \left( S_{\text{ob},k}^{\text{FC,D}}[j] = s_{j,k}^{\text{FC}} | \hat{W}_{\text{RX}_k}[j], \hat{\mathbf{W}}_{\text{FC}_k}^{j-1} \right). \quad (10)$$

We clarify that (9) and (10) can be evaluated by applying the conditional cumulative distribution function (CDF) of the Poisson RV  $S_{\text{ob}}^{\text{RX}_k}[j]$  and the conditional PMF of the Poisson

<sup>3</sup>To decrease the computational complexity at the FC, we consider that the FC assesses the likelihood of the *sum* of  $M_{\text{FC}}$  observations for each  $\text{RX}_k - \text{FC}$  link, which is analogous to L-ML.

RV  $S_{\text{ob},k}^{\text{FC,D}}[j]$ . The conditional means  $\bar{S}_{\text{ob},k}^{\text{FC,D}}[j]$  given  $\hat{\mathbf{W}}_{\text{FC}_k}^{j-1}$  are obtained by replacing  $S_0$ ,  $W_{\text{TX}}[i]$ ,  $P_{\text{ob}}^{(\text{TX}, \text{RX}_k)}$ ,  $M_{\text{RX}}$ ,  $m$ , and  $\Delta t_{\text{RX}}$  in (3) with  $S_{\text{D}}$ ,  $\hat{W}_{\text{FC}_k}[i]$ ,  $P_{\text{ob},k}^{(\text{RX}_k, \text{FC})}$ ,  $M_{\text{FC}}$ ,  $\tilde{m}$ , and  $\Delta t_{\text{FC}}$ , respectively.

2) *SD-ML*: The behavior of each  $\text{RX}_k$  in SD-ML is the same as that in MD-ML, except we assume that each  $\text{RX}_k$  transmits type  $A_1$  molecules to report  $\hat{W}_{\text{RX}_k}[j]$  to the FC. This is because it may not be realistic for each RX to release a unique type of molecule. For simplicity, the number of released type  $A_1$  molecules for each  $\text{RX}_k$  in SD-ML is also denoted by  $S_{\text{D}}$ . The FC receives type  $A_1$  molecules over all  $K$   $\text{RX}_k - \text{FC}$  links and takes  $M_{\text{FC}}$  samples of type  $A_1$  molecules in each symbol interval. The FC adds  $M_{\text{FC}}$  observations for all  $\text{RX}_k - \text{FC}$  links in the  $j$ th symbol interval. We denote  $S_{\text{ob}}^{\text{FC,D}}[j]$  as the total number of  $A_1$  molecules observed within  $V_{\text{FC}}$  in the  $j$ th symbol interval, due to both current and previous emissions of molecules by all RXs. We note that  $S_{\text{ob}}^{\text{FC,D}}[j] = \sum_{k=1}^K S_{\text{ob},k}^{\text{FC,D}}[j]$  is also a Poisson RV whose mean is given by  $\bar{S}_{\text{ob}}^{\text{FC,D}}[j] = \sum_{k=1}^K \bar{S}_{\text{ob},k}^{\text{FC,D}}[j]$ . Values of realizations of  $S_{\text{ob}}^{\text{FC,D}}[j]$  are labeled  $s_j^{\text{FC}}$ . The FC chooses the symbol  $\hat{W}_{\text{FC}}[j]$  that is more likely, given the likelihood of  $s_j^{\text{FC}}$  in the  $j$ th interval. To facilitate the evaluation of  $\mathcal{L}[j]$  for SD-ML, we first define  $\hat{\mathcal{W}}_j^{\text{RX}} = \{\hat{W}_{\text{RX}_1}[j], \dots, \hat{W}_{\text{RX}_K}[j]\}$  as the set of decisions at all RXs in the  $j$ th symbol interval. We then define a set  $\mathcal{R}$  which includes all possible realizations of  $\hat{\mathcal{W}}_j^{\text{RX}}$  and  $|\mathcal{R}| = 2^K$ . Using these notations, we derive  $\mathcal{L}[j]$  as

$$\begin{aligned} \mathcal{L}[j] = \sum_{\substack{\hat{\mathcal{W}}_j^{\text{RX}} \in \mathcal{R} \\ \hat{W}_j^{\text{RX}}}} & \left[ \Pr \left( \hat{\mathcal{W}}_j^{\text{RX}} | W_{\text{TX}}[j], \hat{\mathbf{W}}_{\text{FC}}^{j-1} \right) \right. \\ & \left. \times \Pr \left( S_{\text{ob}}^{\text{FC,D}}[j] = s_j^{\text{FC}} | \hat{\mathcal{W}}_j^{\text{RX}}, \hat{\mathbf{W}}_{\text{FC}_1}^{j-1}, \dots, \hat{\mathbf{W}}_{\text{FC}_K}^{j-1} \right) \right], \quad (11) \end{aligned}$$

where we clarify that we need to consider every realization of  $\hat{\mathcal{W}}_j^{\text{RX}}$  and the corresponding probability leading to  $s_j^{\text{FC}}$ . However, in (11), we note that it is hard for the FC to obtain  $\hat{\mathbf{W}}_{\text{FC}_k}^{j-1}$  when all RXs transmit type  $A_1$  molecules to the FC in SD-ML. Fortunately, due to the symmetric topology,  $\hat{\mathbf{W}}_{\text{FC}_k}^{j-1}$  is not precisely required for calculating the conditional PMF of  $S_{\text{ob}}^{\text{FC,D}}[j]$  in (11); only the number of RXs that transmitted symbol “1” in each previous symbol interval is needed. We first define  $\mathcal{Z}$  as the set where the elements are the possible number of RXs that transmit symbol “1” in each symbol interval, i.e.,  $\mathcal{Z} = \{0, 1, \dots, K\}$ . We denote  $\hat{Z}[j]$  as the FC’s estimate of the number of RXs that transmit symbol “1” in the  $j$ th symbol interval. We define  $\hat{\mathbf{Z}}^l = \{\hat{Z}[1], \dots, \hat{Z}[l]\}$  as the FC’s estimate of the number of RXs transmitting the symbol “1” in the first  $l$  symbol intervals. Hence, for the evaluation of the likelihood in all future intervals, the FC also chooses  $\hat{Z}[j]$  in the  $j$ th interval from the set  $\mathcal{Z}$  that is most likely, given the likelihood of  $s_j^{\text{FC}}$  in the  $j$ th interval.  $\hat{Z}[j]$  is obtained by

$$\hat{Z}[j] = \underset{Z \in \mathcal{Z}}{\operatorname{argmax}} \Pr \left( S_{\text{ob}}^{\text{FC,D}}[j] = s_j^{\text{FC}} | Z, \hat{\mathbf{Z}}^{j-1} \right). \quad (12)$$

Also, since we assume (via symmetry) that the RXs have independent and *identically* distributed observations, we have  $\Pr \left( \hat{W}_{\text{RX}_k}[j] = 1 | W_{\text{TX}}[j], \hat{\mathbf{W}}_{\text{FC}}^{j-1} \right) =$

$\Pr(\hat{W}_{\text{RX}}[j] = 1 | W_{\text{TX}}[j], \hat{\mathbf{W}}_{\text{FC}}^{j-1}) \triangleq \Theta_j$ . Using  $\hat{\mathbf{Z}}^{j-1}$  and the notation  $\Theta_j$ , we rewrite (11) as

$$\begin{aligned} \mathcal{L}[j] &= \sum_{Z=0}^K \binom{K}{Z} \Theta_j^Z (1 - \Theta_j)^{K-Z} \\ &\times \Pr(S_{\text{ob}}^{\text{FC},\text{D}}[j] = s_j^{\text{FC}} | Z, \hat{\mathbf{Z}}^{j-1}), \end{aligned} \quad (13)$$

which can be evaluated by applying the conditional CDF of  $S_{\text{ob}}^{\text{RX}_k}[j]$  and the conditional PMF of  $S_{\text{ob}}^{\text{FC},\text{D}}[j]$ . We now derive the conditional mean of  $S_{\text{ob}}^{\text{FC},\text{D}}[j]$  given  $Z$  and  $\hat{\mathbf{Z}}^{j-1}$ . To this end, we first write  $S_{\text{ob}}^{\text{FC},\text{D}}[j]$  as

$$\begin{aligned} \bar{S}_{\text{ob}}^{\text{FC},\text{D}}[j] &= S_{\text{D}} \sum_{i=1}^{j-1} \sum_{k=1}^K \hat{W}_{\text{FC}_k}[i] \\ &\times \sum_{\tilde{m}=1}^{M_{\text{FC}}} P_{\text{ob},k}^{(\text{RX}_k,\text{FC})} ((j-i)T + \tilde{m}\Delta t_{\text{FC}}) \\ &+ S_{\text{D}} \sum_{k=1}^K \hat{W}_{\text{RX}_k}[j] \sum_{\tilde{m}=1}^{M_{\text{FC}}} P_{\text{ob},k}^{(\text{RX}_k,\text{FC})} (\tilde{m}\Delta t_{\text{FC}}). \end{aligned} \quad (14)$$

Since we consider a symmetric topology, we rewrite (14) as

$$\begin{aligned} \bar{S}_{\text{ob}}^{\text{FC},\text{D}}[j] &= S_{\text{D}} \sum_{i=1}^{j-1} \hat{Z}[i] \sum_{\tilde{m}=1}^{M_{\text{FC}}} P_{\text{ob},k}^{(\text{RX}_k,\text{FC})} ((j-i)T + \tilde{m}\Delta t_{\text{FC}}) \\ &+ S_{\text{D}} Z \sum_{\tilde{m}=1}^{M_{\text{FC}}} P_{\text{ob},k}^{(\text{RX}_k,\text{FC})} (\tilde{m}\Delta t_{\text{FC}}). \end{aligned} \quad (15)$$

3) *SA-ML*: We now detail the second phase for SA-ML. Each RX amplifies the number of molecules observed in the  $j$ th symbol interval, i.e.,  $S_k^{\text{A}}[j] = \alpha S_{\text{ob}}^{\text{RX}_k}[j]$ , where  $S_k^{\text{A}}[j]$  denotes the number of molecules released by  $\text{RX}_k$  in the  $j$ th symbol interval and  $\alpha$  is the *constant* amplification factor at all RXs. All RXs retransmit  $S_k^{\text{A}}[j]$  molecules of type  $A_1$  to the FC at the same time. Since all RXs in both SA-ML and SD-ML release molecules of the same type  $A_1$ , the description of the behavior of the FC in SA-ML is analogous to that in SD-ML. We denote  $S_{\text{ob},k}^{\text{FC},\text{A}}[j]$  as the number of molecules observed within  $V_{\text{FC}}$  in the  $j$ th symbol interval, due to the emissions of molecules from the current and the previous intervals by  $\text{RX}_k$ . The TX –  $\text{RX}_k$  and  $\text{RX}_k$  – FC links are both diffusion-based. Therefore,  $S_{\text{ob},k}^{\text{FC},\text{A}}[j]$  can be accurately approximated by a Poisson RV. We denote  $\bar{S}_{\text{ob},k}^{\text{FC},\text{A}}[j]$  as the mean of  $S_{\text{ob},k}^{\text{FC},\text{A}}[j]$ . The FC adds  $M_{\text{FC}}$  observations for all  $\text{RX}_k$  – FC links in the  $j$ th symbol interval and this sum is denoted by the RV  $S_{\text{ob}}^{\text{FC},\text{A}}[j]$ . We note that  $S_{\text{ob}}^{\text{FC},\text{A}}[j] = \sum_{k=1}^K S_{\text{ob},k}^{\text{FC},\text{A}}[j]$  is also a Poisson RV whose mean is given by  $\bar{S}_{\text{ob}}^{\text{FC},\text{A}}[j] = \sum_{k=1}^K \bar{S}_{\text{ob},k}^{\text{FC},\text{A}}[j]$ . Values of realizations of  $S_{\text{ob}}^{\text{FC},\text{A}}[j]$  are labeled  $s_j^{\text{FC}}$ . The FC chooses the symbol  $\hat{W}_{\text{FC}}[j]$  that is more likely given the likelihood of  $s_j^{\text{FC}}$  in the  $j$ th interval.  $\mathcal{L}[j]$  is given in (16) at the top of the following page, where  $S_{\text{ob}}^{\text{RX}_k}[i]$  and  $s_i^{\text{RX}_k}$ ,  $i \in \{1, \dots, j\}$  and  $k \in \{1, \dots, K\}$ , are defined in Section II-B1 and Section II-B2, respectively. Theoretically, any number of molecules could be observed at each RX. Thus, there are infinite realizations for each Poisson RV  $S_{\text{ob}}^{\text{RX}_k}[i]$  in (16). To enable the evaluation of (16), we consider finitely many random realizations of each Poisson RV

$S_{\text{ob}}^{\text{RX}_k}[i]$ <sup>4</sup>. For example, we generate 5000 random realizations of each  $S_{\text{ob}}^{\text{RX}_k}[i]$  for a given  $\hat{\mathbf{W}}_{\text{FC}}^{j-1}$ , which is sufficient to ensure the accuracy of (16). It is shown that (16) can be evaluated by applying the conditional PMF of the Poisson RV  $S_{\text{ob}}^{\text{FC},\text{A}}[j]$ . We obtain the conditional mean of  $S_{\text{ob},k}^{\text{FC},\text{A}}[j]$  by replacing  $S_0 W_{\text{TX}}[i]$ ,  $P_{\text{ob}}^{(\text{TX},\text{RX}_k)}$ ,  $M_{\text{RX}}$ ,  $m$ , and  $\Delta t_{\text{RX}}$  in (3) with  $S_k^{\text{A}}[j]$ ,  $P_{\text{ob},k}^{(\text{RX}_k,\text{FC})}$ ,  $M_{\text{FC}}$ ,  $\tilde{m}$ , and  $\Delta t_{\text{FC}}$ , respectively. Based on  $\bar{S}_{\text{ob}}^{\text{FC},\text{A}}[j] = \sum_{k=1}^K \bar{S}_{\text{ob},k}^{\text{FC},\text{A}}[j]$ , we can then obtain the conditional mean of  $S_{\text{ob}}^{\text{FC},\text{A}}[j]$ .

#### IV. ERROR PERFORMANCE ANALYSIS

In this section, we derive the error probability of the cooperative MC system in the  $j$ th symbol interval using the *genie-aided history*, which leads to tractable expressions. We denote  $Q_{\text{FC}}[j]$  as the error probability of the cooperative MC system in the  $j$ th symbol interval for a TX sequence  $\mathbf{W}_{\text{TX}}^{j-1}$ . To this end, we first present the lower-complexity decision rules for L-ML, SD-ML, and SA-ML, compared to the general decision rule in (5) and (6). Based on these decision rules, we derive  $Q_{\text{FC}}[j]$  for L-ML in perfect reporting and SD-ML and SA-ML in noisy reporting using the genie-aided history. We note that the error performance of F-ML and MD-ML is mathematically intractable. By averaging  $Q_{\text{FC}}[j]$  over all symbol intervals and all possible realizations of  $\mathbf{W}_{\text{TX}}^{j-1}$ , the average error probability of the cooperative MC system,  $\bar{Q}_{\text{FC}}$ , can be obtained.

Throughout this section, we need to consider the case where all previously-transmitted symbols are “0” as a special case in the derivation of decision rules and corresponding error probabilities, since the denominators in decision rules cannot be 0. Although some decision rules may appear to be forms similar to those in [22], [23], their results cannot be directly applied to this paper, since [22], [23] only considered one-phase RX-FC links for event detection.

##### A. Perfect Reporting

In this subsection, we analyze the error performance of L-ML with the genie-aided history to provide an analytical lower bound on the achievable error performance of the system with *either* perfect or noisy reporting.

1) *L-ML*: We now derive  $Q_{\text{FC}}[j]$  in the perfect reporting scenario for L-ML. We define  $\lambda_{n,k}[j]$  as the expected ISI at  $\text{RX}_k$  in the  $j$ th symbol interval due to the previously-transmitted TX symbols  $\mathbf{W}_{\text{TX}}^{j-1}$ , i.e.,

$$\lambda_{n,k}[j] = \sum_{i=1}^{j-1} S_0 W_{\text{TX}}[i] \sum_{m=1}^{M_{\text{RX}}} P_{\text{ob}}^{(\text{TX},\text{RX}_k)} ((j-i)T + m\Delta t_{\text{RX}}). \quad (17)$$

We define  $\lambda_{s,k}[j]$  as the number of signal molecules at  $\text{RX}_k$  in the  $j$ th symbol interval due to the currently-transmitted TX symbol  $W_{\text{TX}}[j] = 1$ , i.e.,

$$\lambda_{s,k}[j] = S_0 \sum_{m=1}^{M_{\text{RX}}} P_{\text{ob}}^{(\text{TX},\text{RX}_k)} (m\Delta t_{\text{RX}}). \quad (18)$$

<sup>4</sup>We assume that the FC may have sufficiently high computational capabilities such that it can generate random realizations. This assumption is because the FC could have a direct interface with computational resources.

$$\begin{aligned}
\mathcal{L}[j] = & \sum_{s_1^{\text{RX}_1}=0}^{\infty} \dots \sum_{s_j^{\text{RX}_1}=0}^{\infty} \dots \sum_{s_1^{\text{RX}_K}=0}^{\infty} \dots \sum_{s_j^{\text{RX}_K}=0}^{\infty} \Pr(S_{\text{ob}}^{\text{RX}_1}[1] = s_1^{\text{RX}_1}, \dots, S_{\text{ob}}^{\text{RX}_1}[j] = s_j^{\text{RX}_1}, \dots, \\
& S_{\text{ob}}^{\text{RX}_K}[1] = s_1^{\text{RX}_K}, \dots, S_{\text{ob}}^{\text{RX}_K}[j] = s_j^{\text{RX}_K} | W_{\text{TX}}[j], \hat{\mathbf{W}}_{\text{FC}}^{j-1}) \Pr(S_{\text{ob}}^{\text{FC},\text{A}}[j] = s_j^{\text{FC}} \\
& | S_{\text{ob}}^{\text{RX}_1}[1] = s_1^{\text{RX}_1}, \dots, S_{\text{ob}}^{\text{RX}_1}[j] = s_j^{\text{RX}_1}, \dots, S_{\text{ob}}^{\text{RX}_K}[1] = s_1^{\text{RX}_K}, \dots, S_{\text{ob}}^{\text{RX}_K}[j] = s_j^{\text{RX}_K})
\end{aligned} \quad (16)$$

We note that the conditional mean of  $S_{\text{ob}}^{\text{RX}_k}[j]$  given  $\hat{\mathbf{W}}_{\text{TX}}^{j-1}$  is  $\lambda_{s,k}[j] + \lambda_{n,k}[j]$  and  $\lambda_{n,k}[j]$  when the  $j$ th symbol transmitted by the TX is  $W_{\text{TX}}[j] = 1$  and  $W_{\text{TX}}[j] = 0$ , respectively. If not all the previous symbols transmitted by the TX are “0”, i.e.,  $\hat{\mathbf{W}}_{\text{TX}}^{j-1} \neq \mathbf{0}$ , then we have  $\lambda_{n,k}[j] > 0$ . If all previous symbols transmitted by the TX are “0”, i.e.,  $\hat{\mathbf{W}}_{\text{TX}}^{j-1} = \mathbf{0}$ , then we have  $\lambda_{n,k}[j] = 0$ . Since we assume (via symmetry) that the RXs have independent and identically distributed observations, we have  $\lambda_{n,k}[j] = \lambda_n[j]$  and  $\lambda_{s,k}[j] = \lambda_s[j]$ . For the sake of brevity, for L-ML, we define  $\mathcal{L}[j | W_{\text{TX}}[j] = 1, \hat{\mathbf{W}}_{\text{TX}}^{j-1}] \triangleq \mathcal{L}_1$  and  $\mathcal{L}[j | W_{\text{TX}}[j] = 0, \hat{\mathbf{W}}_{\text{TX}}^{j-1}] \triangleq \mathcal{L}_0$ . Applying the conditional PMF of the Poisson RV  $S_{\text{ob}}^{\text{RX}_k}[j]$  to (8), we write  $\mathcal{L}_1$  and  $\mathcal{L}_0$  as

$$\mathcal{L}_1 = \prod_{k=1}^K \left[ \frac{(\lambda_s[j] + \lambda_n[j])^{s_j^{\text{RX}_k}}}{s_j^{\text{RX}_k}!} \exp(-(\lambda_s[j] + \lambda_n[j])) \right] \quad (19)$$

and

$$\mathcal{L}_0 = \prod_{k=1}^K \left[ \frac{(\lambda_n[j])^{s_j^{\text{RX}_k}}}{s_j^{\text{RX}_k}!} \exp(-\lambda_n[j]) \right], \quad (20)$$

respectively. Based on (19) and (20), we rewrite the general decision rule of L-ML in (5) as a lower-complexity decision rule in the following theorem.

*Theorem 1:* When  $\lambda_n[j] > 0$ , the decision rule of L-ML is  $\hat{W}_{\text{FC}}[j] = 1$  if  $s_j^{\text{RX}} \geq \xi_{\text{FC}}^{\text{ad}}[j]$ , otherwise  $\hat{W}_{\text{FC}}[j] = 0$ , where  $s_j^{\text{RX}} = \sum_{k=1}^K s_j^{\text{RX}_k}$  and  $\xi_{\text{FC}}^{\text{ad}}[j] = [K\lambda_s[j]/\log((\lambda_s[j] + \lambda_n[j])/(\lambda_n[j]))]$ . When  $\lambda_n[j] = 0$ , the decision rule of L-ML is  $\hat{W}_{\text{FC}}[j] = 1$  if  $s_j^{\text{RX}} > 0$  and  $\hat{W}_{\text{FC}}[j] = 0$  if  $s_j^{\text{RX}} = 0$ .

*Proof:* Applying (19) and (20) to (5), we write the decision rule of L-ML as

$$\frac{(\lambda_s[j] + \lambda_n[j])^{s_j^{\text{RX}}}}{\exp(K(\lambda_s[j] + \lambda_n[j]))} \hat{W}_{\text{FC}}[j]=1 \geq \frac{(\lambda_n[j])^{s_j^{\text{RX}}}}{\exp(K\lambda_n[j])}. \quad (21)$$

When  $\lambda_n[j] > 0$ , we further write (21) as

$$\left( \frac{(\lambda_s[j] + \lambda_n[j])}{\lambda_n[j]} \right)^{s_j^{\text{RX}}} \hat{W}_{\text{FC}}[j]=1 \geq \exp(K\lambda_s[j]). \quad (22)$$

We rearrange (22) and obtain the decision rule of L-ML when  $\lambda_n[j] > 0$ . If  $\lambda_n[j] = 0$  and  $s_j^{\text{RX}} = 0$ , we write (21) as  $\exp(-K\lambda_s[j]) < 1$ , where the decision at the FC is always  $\hat{W}_{\text{FC}}[j] = 0$ . If  $\lambda_n[j] = 0$  and  $s_j^{\text{RX}} > 0$ , we write (21) as  $(\lambda_s[j])^{s_j^{\text{RX}}} \exp(-K\lambda_s[j]) > 0$ , where the decision at the FC is always  $\hat{W}_{\text{FC}}[j] = 1$ . This completes the proof.  $\blacksquare$

Based on Theorem 1, when  $\hat{\mathbf{W}}_{\text{TX}}^{j-1} \neq \mathbf{0}$ , we evaluate  $Q_{\text{FC}}[j]$  for L-ML as

$$\begin{aligned}
Q_{\text{FC}}[j] = & (1 - P_1) \Pr(S_{\text{ob}}^{\text{RX}}[j] \geq \xi_{\text{FC}}^{\text{ad}}[j] | W_{\text{TX}}[j] = 0, \hat{\mathbf{W}}_{\text{TX}}^{j-1}) \\
& + P_1 \Pr(S_{\text{ob}}^{\text{RX}}[j] < \xi_{\text{FC}}^{\text{ad}}[j] | W_{\text{TX}}[j] = 1, \hat{\mathbf{W}}_{\text{TX}}^{j-1}),
\end{aligned} \quad (23)$$

where  $S_{\text{ob}}^{\text{RX}}[j] = \sum_{k=1}^K S_{\text{ob}}^{\text{RX}_k}[j]$ . When  $\hat{\mathbf{W}}_{\text{TX}}^{j-1} = \mathbf{0}$ ,  $Q_{\text{FC}}[j]$  for L-ML can be obtained by replacing  $\geq$ ,  $<$ , and  $\xi_{\text{FC}}^{\text{ad}}[j]$  with  $>$ ,  $=$ , and 0 in (23), respectively.

*Remark 1:* If the FC instead adds all RXs’  $KM_{\text{RX}}$  observations in the  $j$ th symbol interval to obtain the single sum  $s_j^{\text{RX}}$  in the  $j$ th symbol interval, it can be shown that the error performance of the FC is actually the *same* as that of L-ML. That is, the knowledge of individual  $s_j^{\text{RX}_k}$  for each RX does *not* improve detection performance over only knowing the sum  $s_j^{\text{RX}}$ .

### B. Noisy Reporting

In this subsection, we analyze the error performance of SD-ML and SA-ML with the genie-aided history. We note that the closed-form expression of  $Q_{\text{FC}}[j]$  for SD-ML is mathematically tractable when one RX exists in the system, i.e.,  $K = 1$ .

1) *SD-ML:* We now derive  $Q_{\text{FC}}[j]$  for the SD-ML variant. To this end, we first define  $\hat{\lambda}_{\text{N}}^{\text{D}}[j]$  as the expected ISI at the FC in the  $j$ th symbol interval due to the previous symbols transmitted by all RXs,  $\hat{\mathbf{W}}_{\text{RX}_1}^{j-1}, \hat{\mathbf{W}}_{\text{RX}_2}^{j-1}, \dots, \hat{\mathbf{W}}_{\text{RX}_K}^{j-1}$ , i.e.,

$$\hat{\lambda}_{\text{N}}^{\text{D}}[j] = S_{\text{D}} \sum_{i=1}^{j-1} \sum_{k=1}^K \hat{W}_{\text{RX}_k}[i] \sum_{\tilde{m}=1}^{M_{\text{FC}}} P_{\text{ob},k}^{(\text{RX}_k, \text{FC})} ((j-i)T + \tilde{m}\Delta t_{\text{FC}}). \quad (24)$$

We then define  $\hat{\lambda}_{s,k}^{\text{D}}[j]$  as the number of signal molecules at the FC in the  $j$ th symbol interval due to the currently-transmitted RX<sub>k</sub> symbol  $\hat{W}_{\text{RX}_k}[j] = 1$ , i.e.,

$$\hat{\lambda}_{s,k}^{\text{D}}[j] = S_{\text{D}} \sum_{\tilde{m}=1}^{M_{\text{FC}}} P_{\text{ob},k}^{(\text{RX}_k, \text{FC})} (\tilde{m}\Delta t_{\text{FC}}), \quad (25)$$

where we have  $\hat{\lambda}_{s,k}^{\text{D}}[j] = \hat{\lambda}_s^{\text{D}}[j]$ , since we consider a cooperative system with a symmetric topology. We note that the conditional mean of  $S_{\text{ob}}^{\text{FC},\text{D}}[j]$  given the previously-transmitted symbols by all RXs,  $\hat{\mathbf{W}}_{\text{RX}_1}^{j-1}, \hat{\mathbf{W}}_{\text{RX}_2}^{j-1}, \dots, \hat{\mathbf{W}}_{\text{RX}_K}^{j-1}$ , is  $\hat{\lambda}_{\text{N}}^{\text{D}}[j] + Z\hat{\lambda}_s^{\text{D}}[j]$  when the number of the RXs transmitting symbol “1” in the  $j$ th symbol interval is  $Z$ . If not all previous symbols transmitted by all RXs are “0”, i.e.,  $\sum_{i=1}^{j-1} \sum_{k=1}^K \hat{W}_{\text{RX}_k}[i] \neq 0$ , then we have  $\hat{\lambda}_{\text{N}}^{\text{D}}[j] > 0$ . If all previous symbols transmitted

by all RXs are “0”, i.e.,  $\sum_{i=1}^{j-1} \sum_{k=1}^K \hat{W}_{\text{RX}_k}[i] = 0$ , then we have  $\hat{\lambda}_{\text{N}}^{\text{D}}[j] = 0$ . We then denote  $P_{\text{md},k}[j]$  and  $P_{\text{fa},k}[j]$  as the expected miss detection probability and the expected false alarm probability of the TX – RX<sub>k</sub> link in the  $j$ th symbol interval for given  $\mathbf{W}_{\text{TX}}^{j-1}$ , respectively; see [14]. Due to symmetry in the system’s topology, we have  $P_{\text{md},k}[j] = P_{\text{md}}[j]$  and  $P_{\text{fa},k}[j] = P_{\text{fa}}[j]$ . For the sake of brevity, for SD-ML, we define  $\mathcal{L} \left[ j | W_{\text{TX}}[j] = 1, \mathbf{W}_{\text{TX}}^{j-1}, \hat{\mathbf{W}}_{\text{RX}_k}^{j-1} \right] \triangleq \mathcal{L}_1^{\text{SD}}[j]$  and  $\mathcal{L} \left[ j | W_{\text{TX}}[j] = 0, \mathbf{W}_{\text{TX}}^{j-1}, \hat{\mathbf{W}}_{\text{RX}_k}^{j-1} \right] \triangleq \mathcal{L}_0^{\text{SD}}[j]$ . Applying the conditional PMF of  $S_{\text{ob}}^{\text{FC},\text{D}}[j]$  to (13), we write  $\mathcal{L}_1^{\text{SD}}[j]$  and  $\mathcal{L}_0^{\text{SD}}[j]$  as

$$\begin{aligned} \mathcal{L}_1^{\text{SD}}[j] &= \sum_{Z=0}^K \left[ \binom{K}{Z} (1 - P_{\text{md}}[j])^Z (P_{\text{md}}[j])^{K-Z} (s_j^{\text{FC}}!)^{-1} \right. \\ &\quad \times \exp \left( -\hat{\lambda}_{\text{N}}^{\text{D}}[j] - Z \hat{\lambda}_{\text{s}}^{\text{D}}[j] \right) \left( \hat{\lambda}_{\text{N}}^{\text{D}}[j] + Z \hat{\lambda}_{\text{s}}^{\text{D}}[j] \right)^{s_j^{\text{FC}}} \left. \right] \end{aligned} \quad (26)$$

and

$$\begin{aligned} \mathcal{L}_0^{\text{SD}}[j] &= \sum_{Z=0}^K \left[ \binom{K}{Z} P_{\text{fa}}[j]^Z (1 - P_{\text{fa}}[j])^{K-Z} (s_j^{\text{FC}}!)^{-1} \right. \\ &\quad \times \exp \left( -\hat{\lambda}_{\text{N}}^{\text{D}}[j] - Z \hat{\lambda}_{\text{s}}^{\text{D}}[j] \right) \left( \hat{\lambda}_{\text{N}}^{\text{D}}[j] + Z \hat{\lambda}_{\text{s}}^{\text{D}}[j] \right)^{s_j^{\text{FC}}} \left. \right], \end{aligned} \quad (27)$$

respectively. Based on (26) and (27), we rewrite the general decision rule of SD-ML in (6) as a lower-complexity decision rule in the following theorem.

**Theorem 2:** When  $\hat{\lambda}_{\text{N}}^{\text{D}}[j] > 0$ , the decision rule of SD-ML is  $\hat{W}_{\text{FC}}[j] = 1$  if  $s_j^{\text{FC}} \geq \xi_{\text{FC}}^{\text{ad},\text{SD}}[j]$ , otherwise  $\hat{W}_{\text{FC}}[j] = 0$ , where  $\xi_{\text{FC}}^{\text{ad},\text{SD}}[j]$  is the solution to the equation  $\mathcal{L}_1^{\text{SD}}[j] = \mathcal{L}_0^{\text{SD}}[j]$ . We note that this equation has a real-valued solution only when  $\hat{\lambda}_{\text{N}}^{\text{D}}[j] > 0$ . When  $\hat{\lambda}_{\text{N}}^{\text{D}}[j] = 0$ , the decision rule for SD-ML is  $\hat{W}_{\text{FC}}[j] = 1$  if  $s_j^{\text{FC}} > 0$  and  $\hat{W}_{\text{FC}}[j] = 0$  if  $s_j^{\text{FC}} = 0$ .

*Proof:* The proof of Theorem 2 is given in the Appendix.  $\blacksquare$

Based on Theorem 2, when  $\hat{\lambda}_{\text{N}}^{\text{D}}[j] > 0$ , we evaluate the conditional  $Q_{\text{FC}}$  as

$$\begin{aligned} Q_{\text{FC}} \left[ j | \hat{\lambda}_{\text{N}}^{\text{D}}[j] > 0 \right] &= P_1 \Pr \left( S_{\text{ob}}^{\text{FC},\text{D}}[j] < \xi_{\text{FC}}^{\text{ad},\text{SD}}[j] | W_{\text{TX}}[j] = 1, \hat{\lambda}_{\text{N}}^{\text{D}}[j] > 0 \right) \\ &\quad + (1 - P_1) \Pr \left( S_{\text{ob}}^{\text{FC},\text{D}}[j] \geq \xi_{\text{FC}}^{\text{ad},\text{SD}}[j] | W_{\text{TX}}[j] = 0, \hat{\lambda}_{\text{N}}^{\text{D}}[j] > 0 \right), \end{aligned} \quad (28)$$

where the conditional CDF of the Poisson RV  $S_{\text{ob}}^{\text{FC},\text{D}}[j]$  can be evaluated by

$$\begin{aligned} \Pr \left( S_{\text{ob}}^{\text{FC},\text{D}}[j] < \xi_{\text{FC}}^{\text{ad},\text{SD}}[j] | W_{\text{TX}}[j], \hat{\lambda}_{\text{N}}^{\text{D}}[j] \right) &= \sum_{Z=0}^{\xi_{\text{FC}}^{\text{ad},\text{SD}}[j]-1} \left[ \binom{K}{Z} \Theta_j^Z (1 - \Theta_j)^{K-Z} \exp \left( -\hat{\lambda}_{\text{N}}^{\text{D}}[j] + Z \hat{\lambda}_{\text{s}}^{\text{D}}[j] \right) \right. \\ &\quad \times \left. \sum_{\eta=0}^{\xi_{\text{FC}}^{\text{ad},\text{SD}}[j]-1} \left( \hat{\lambda}_{\text{N}}^{\text{D}}[j] + Z \hat{\lambda}_{\text{s}}^{\text{D}}[j] \right)^{\eta} / (\eta!) \right]. \end{aligned} \quad (29)$$

In (29),  $\Theta_j$  is defined in Section III-B2 and  $\hat{\lambda}_{\text{N}}^{\text{D}}[j]$  can be evaluated by (24) via approximated  $\hat{\mathbf{W}}_{\text{RX}_k}^{j-1}$ ,  $k \in \{1, 2, \dots, K\}$ . The approximated  $\hat{\mathbf{W}}_{\text{RX}_k}^{j-1}$  can be obtained using the biased coin toss method introduced in [31]. Specifically, we model the  $i$ th decision at RX<sub>k</sub>,  $\hat{W}_{\text{RX}_k}[i]$ , as  $\hat{W}_{\text{RX}_k}[i] = |\lambda - W_{\text{TX}}[i]|$ , where  $i \in \{1, \dots, j-1\}$  and  $\lambda \in \{0, 1\}$  is the outcome of the coin toss with  $\Pr(\lambda = 1) = P_{\text{md}}[i]$  if  $W_{\text{TX}}[i] = 1$  and  $\Pr(\lambda = 1) = P_{\text{fa}}[i]$  if  $W_{\text{TX}}[i] = 0$ . When  $\hat{\lambda}_{\text{N}}^{\text{D}}[j] = 0$ , we evaluate the conditional  $Q_{\text{FC}}$  as

$$\begin{aligned} Q_{\text{FC}} \left[ j | \hat{\lambda}_{\text{N}}^{\text{D}}[j] = 0 \right] &= P_1 \Pr \left( S_{\text{ob}}^{\text{FC},\text{D}}[j] = 0 | W_{\text{TX}}[j] = 1, \hat{\lambda}_{\text{N}}^{\text{D}}[j] = 0 \right) \\ &\quad + (1 - P_1) \Pr \left( S_{\text{ob}}^{\text{FC},\text{D}}[j] > 0 | W_{\text{TX}}[j] = 0, \hat{\lambda}_{\text{N}}^{\text{D}}[j] = 0 \right), \end{aligned} \quad (30)$$

where the conditional CDF of the Poisson RV  $S_{\text{ob}}^{\text{FC},\text{D}}[j]$  can be evaluated analogously to (29). Combining (30) and (28), we obtain  $Q_{\text{FC}}[j]$  for SD-ML as

$$\begin{aligned} Q_{\text{FC}}[j] &= \Pr \left( \hat{\lambda}_{\text{N}}^{\text{D}}[j] > 0 | \mathbf{W}_{\text{TX}}^{j-1} \right) Q_{\text{FC}} \left[ j | \hat{\lambda}_{\text{N}}^{\text{D}}[j] > 0 \right] \\ &\quad + \Pr \left( \hat{\lambda}_{\text{N}}^{\text{D}}[j] = 0 | \mathbf{W}_{\text{TX}}^{j-1} \right) Q_{\text{FC}} \left[ j | \hat{\lambda}_{\text{N}}^{\text{D}}[j] = 0 \right]. \end{aligned} \quad (31)$$

Finally, we derive the analytical closed-form expression for  $Q_{\text{FC}}[j]$  for SD-ML with  $K = 1$ . When  $K = 1$ , we write (26) and (27) as

$$\begin{aligned} \mathcal{L}_1^{\text{SD}}[j] &= \left( P_{\text{md}}[j] \exp \left( -\hat{\lambda}_{\text{N}}^{\text{D}}[j] \right) \left( \hat{\lambda}_{\text{N}}^{\text{D}}[j] \right)^{s_j^{\text{FC}}} \right. \\ &\quad + (1 - P_{\text{md}}[j]) \exp \left( -\hat{\lambda}_{\text{N}}^{\text{D}}[j] - \hat{\lambda}_{\text{s}}^{\text{D}}[j] \right) \\ &\quad \times \left. \left( \hat{\lambda}_{\text{N}}^{\text{D}}[j] + \hat{\lambda}_{\text{s}}^{\text{D}}[j] \right)^{s_j^{\text{FC}}} \right) / (s_j^{\text{FC}}!) \end{aligned} \quad (32)$$

and

$$\begin{aligned} \mathcal{L}_0^{\text{SD}}[j] &= \left( (1 - P_{\text{fa}}[j]) \exp \left( -\hat{\lambda}_{\text{N}}^{\text{D}}[j] \right) \left( \hat{\lambda}_{\text{N}}^{\text{D}}[j] \right)^{s_j^{\text{FC}}} \right. \\ &\quad + P_{\text{fa}}[j] \exp \left( -\hat{\lambda}_{\text{N}}^{\text{D}}[j] - \hat{\lambda}_{\text{s}}^{\text{D}}[j] \right) \\ &\quad \times \left. \left( \hat{\lambda}_{\text{N}}^{\text{D}}[j] + \hat{\lambda}_{\text{s}}^{\text{D}}[j] \right)^{s_j^{\text{FC}}} \right) / (s_j^{\text{FC}}!), \end{aligned} \quad (33)$$

respectively. Substituting (32) and (33) into  $\mathcal{L}_1^{\text{SD}}[j] = \mathcal{L}_0^{\text{SD}}[j]$  and solving the equation in terms of  $\xi_{\text{FC}}^{\text{ad},\text{SD}}[j]$ , we obtain the closed-form expression for  $\xi_{\text{FC}}^{\text{ad},\text{SD}}[j]$  when  $K = 1$  as

$$\xi_{\text{FC}}^{\text{ad},\text{SD}}[j] = \left\lfloor \left( \hat{\lambda}_{\text{s}}^{\text{D}}[j] \right) / \log \left( \left( \hat{\lambda}_{\text{N}}^{\text{D}}[j] + \hat{\lambda}_{\text{s}}^{\text{D}}[j] \right) / \hat{\lambda}_{\text{N}}^{\text{D}}[j] \right) \right\rfloor. \quad (34)$$

We note that  $Q_{\text{FC}}[j]$  for SD-ML with  $K = 1$  can be obtained using (31) via (34).

2) **SA-ML:** We now derive  $Q_{\text{FC}}[j]$  in the noisy reporting scenario for SA-ML. In (16), multiple possible realizations of each Poisson RV  $S_{\text{ob}}^{\text{RX}_k}[i]$  make the analytical error performance analysis cumbersome. To tackle this cumbersomeness, we consider only one random realization of  $S_{\text{ob}}^{\text{RX}_k}[i]$  with the mean  $\bar{S}_{\text{ob}}^{\text{RX}_k}[i]$  for the given previous symbols transmitted by the TX,  $\mathbf{W}_{\text{TX}}^{j-1}$ . We define  $\hat{\lambda}_{\text{N}}^{\text{A}}[j]$  as the expected ISI at the FC in the  $j$ th symbol interval due to  $\mathbf{W}_{\text{TX}}^{j-1}$ . We define  $\hat{\lambda}_{\text{s}}^{\text{A}}[j]$  as the number of the signal molecules at the FC in the  $j$ th symbol interval

due to  $W_{\text{TX}}[j] = 1$ . By modeling the realization of  $S_{\text{ob}}^{\text{RX}_k}[i]$  as its mean  $\bar{S}_{\text{ob}}^{\text{RX}_k}[i]$ , we write  $\hat{\lambda}_{\text{N}}^{\text{A}}[j]$  and  $\hat{\lambda}_{\text{S}}^{\text{A}}[j]$  as

$$\begin{aligned} \hat{\lambda}_{\text{N}}^{\text{A}}[j] &= \sum_{k=1}^K \left( \sum_{i=1}^{j-1} \alpha \bar{S}_{\text{ob}}^{\text{RX}_k}[i] \sum_{m=1}^{M_{\text{FC}}} P_{\text{ob},k}^{(\text{RX}_k, \text{FC})} ((j-i)T + \tilde{m}\Delta t_{\text{FC}}) \right. \\ &\quad + \alpha S_0 \sum_{i=1}^{j-1} W_{\text{TX}}[i] \sum_{m=1}^{M_{\text{RX}}} P_{\text{ob}}^{(\text{TX}, \text{RX})} ((j-i)T + m\Delta t_{\text{RX}}) \\ &\quad \left. \times \sum_{m=1}^{M_{\text{FC}}} P_{\text{ob},k}^{(\text{RX}_k, \text{FC})} (\tilde{m}\Delta t_{\text{FC}}) \right) \quad (35) \end{aligned}$$

and

$$\hat{\lambda}_{\text{S}}^{\text{A}}[j] = \sum_{k=1}^K \alpha S_0 \sum_{m=1}^{M_{\text{RX}}} P_{\text{ob}}^{(\text{TX}, \text{RX})} (m\Delta t_{\text{RX}}) \sum_{m=1}^{M_{\text{FC}}} P_{\text{ob},k}^{(\text{RX}_k, \text{FC})} (\tilde{m}\Delta t_{\text{FC}}), \quad (36)$$

respectively.  $\hat{\lambda}_{\text{N}}^{\text{A}}[j]$  in (35) consists of two components. The first summation over  $i$  is the expected ISI at the FC in the  $j$ th symbol interval due to the molecules released by the RXs but without the amplification of the RXs' ISI from the TX. The second summation over  $i$  accounts for the amplification of the ISI in the  $j$ th symbol interval at all RXs due to  $\mathbf{W}_{\text{TX}}^{j-1}$ . We note that the conditional mean of  $S_{\text{ob}}^{\text{FC}, \text{A}}[j]$  is  $\hat{\lambda}_{\text{S}}^{\text{A}}[j] + \hat{\lambda}_{\text{N}}^{\text{A}}[j]$  when  $W_{\text{TX}}[j] = 1$ , and the conditional mean of  $S_{\text{ob}}^{\text{FC}, \text{A}}[j]$  is  $\hat{\lambda}_{\text{N}}^{\text{A}}[j]$  when  $W_{\text{TX}}[j] = 0$ . If not all previous symbols transmitted by the TX are “0”, i.e.,  $\mathbf{W}_{\text{TX}}^{j-1} \neq \mathbf{0}$ , then we have  $\hat{\lambda}_{\text{N}}^{\text{A}}[j] > 0$ . If all previous symbols transmitted by the TX are “0”, i.e.,  $\mathbf{W}_{\text{TX}}^{j-1} = \mathbf{0}$ , then we have  $\hat{\lambda}_{\text{N}}^{\text{A}}[j] = 0$ . For the sake of brevity, for SA-ML, we define  $\mathcal{L}[j|W_{\text{TX}}[j] = 1, \mathbf{W}_{\text{TX}}^{j-1}] \triangleq \mathcal{L}_1^{\text{SA}}$  and  $\mathcal{L}[j|W_{\text{TX}}[j] = 0, \mathbf{W}_{\text{TX}}^{j-1}] \triangleq \mathcal{L}_0^{\text{SA}}$ . Applying the conditional PMF of the Poisson RV  $S_{\text{ob}}^{\text{FC}, \text{A}}[j]$  to (16), we derive  $\mathcal{L}_1^{\text{SA}}$  and  $\mathcal{L}_0^{\text{SA}}$  as

$$\mathcal{L}_1^{\text{SA}} = \frac{\left(\hat{\lambda}_{\text{S}}^{\text{A}}[j] + \hat{\lambda}_{\text{N}}^{\text{A}}[j]\right)^{s_j^{\text{FC}}}}{s_j^{\text{FC}}!} \exp\left(-\left(\hat{\lambda}_{\text{S}}^{\text{A}}[j] + \hat{\lambda}_{\text{N}}^{\text{A}}[j]\right)\right) \quad (37)$$

and

$$\mathcal{L}_0^{\text{SA}} = \frac{\left(\hat{\lambda}_{\text{N}}^{\text{A}}[j]\right)^{s_j^{\text{FC}}}}{s_j^{\text{FC}}!} \exp\left(-\hat{\lambda}_{\text{N}}^{\text{A}}[j]\right), \quad (38)$$

respectively. Based on (37) and (38), we rewrite the general decision rule of SA-ML in (5) as a lower-complexity decision rule in the following theorem.

**Theorem 3:** When  $\hat{\lambda}_{\text{N}}^{\text{A}}[j] > 0$ , the decision rule of SA-ML is  $\hat{W}_{\text{FC}}[j] = 1$  if  $s_j^{\text{FC}} \geq \xi_{\text{FC}}^{\text{ad}, \text{SA}}[j]$ , otherwise  $\hat{W}_{\text{FC}}[j] = 0$ .  $\xi_{\text{FC}}^{\text{ad}, \text{SA}}[j]$  can be obtained by replacing  $\hat{\lambda}_{\text{S}}^{\text{A}}[j]$  and  $\hat{\lambda}_{\text{N}}^{\text{A}}[j]$  with  $\hat{\lambda}_{\text{S}}^{\text{A}}[j]$  and  $\hat{\lambda}_{\text{N}}^{\text{A}}[j]$  in (34), respectively. When  $\hat{\lambda}_{\text{N}}^{\text{A}}[j] = 0$ , the decision rule for SA-ML is  $\hat{W}_{\text{FC}}[j] = 1$  if  $s_j^{\text{FC}} > 0$  and  $\hat{W}_{\text{FC}}[j] = 0$  if  $s_j^{\text{FC}} = 0$ .

*Proof:* Theorem 3 can be proven analogously to the proof of Theorem 1.  $\blacksquare$

Based on Theorem 3, when  $\mathbf{W}_{\text{TX}}^{j-1} \neq \mathbf{0}$ , we evaluate  $Q_{\text{FC}}[j]$  for SA-ML as

$$\begin{aligned} Q_{\text{FC}}[j] &= (1 - P_1) \Pr(S_{\text{ob}}^{\text{FC}, \text{A}}[j] \geq \xi_{\text{FC}}^{\text{ad}, \text{SA}}[j] | W_{\text{TX}}[j] = 0, \mathbf{W}_{\text{TX}}^{j-1}) \\ &\quad + P_1 \Pr(S_{\text{ob}}^{\text{FC}, \text{A}}[j] < \xi_{\text{FC}}^{\text{ad}, \text{SA}}[j] | W_{\text{TX}}[j] = 1, \mathbf{W}_{\text{TX}}^{j-1}), \quad (39) \end{aligned}$$

TABLE II  
ENVIRONMENTAL PARAMETERS

Parameter	Symbol	Value
Radius of RXs	$r_{\text{RX}_k}$	$0.2 \mu\text{m}$
Radius of FC	$r_{\text{FC}}$	$0.2 \mu\text{m}$
Time step at RXs	$\Delta t_{\text{RX}}$	$100 \mu\text{s}$
Time step at FC	$\Delta t_{\text{FC}}$	$30 \mu\text{s}$
Number of samples by RXs	$M_{\text{RX}}$	5
Number of samples by FC	$M_{\text{FC}}$	10
Transmission time interval	$t_{\text{trans}}$	1 ms
Report time interval	$t_{\text{report}}$	0.3 ms
Bit interval time	$T$	1.3 ms
Diffusion coefficient	$D_0 = D_k$	$5 \times 10^{-9} \text{m}^2/\text{s}$
Length of symbol sequence	$L$	20
Probability of binary 1	$P_1$	0.5

TABLE III  
DEVICES' LOCATION

Devices	X-axis [ $\mu\text{m}$ ]	Y-axis [ $\mu\text{m}$ ]	Z-axis [ $\mu\text{m}$ ]
TX	0	0	0
RX <sub>1</sub>	2	0.6	0
RX <sub>2</sub>	2	-0.6	0
RX <sub>3</sub>	2	-0.3	0.5196
RX <sub>4</sub>	2	-0.3	-0.519
RX <sub>5</sub>	2	0.3	0.5196
RX <sub>6</sub>	2	0.3	-0.5196
FC	2	0	0

where  $\Pr(S_{\text{ob}}^{\text{FC}, \text{A}}[j] < \xi_{\text{FC}}^{\text{ad}, \text{SA}}[j] | \mathbf{W}_{\text{TX}}^j)$  can be evaluated by replacing  $\hat{\mathbf{W}}_{\text{FC}}^{j-1}$  and  $S_{\text{ob}}^{\text{FC}, \text{A}}[j] = s_j^{\text{FC}}$  in (16) with  $\mathbf{W}_{\text{TX}}^{j-1}$  and  $S_{\text{ob}}^{\text{FC}, \text{A}}[j] < \xi_{\text{FC}}^{\text{ad}, \text{SA}}[j]$ , respectively. Similar to the evaluation of (16), we consider finitely many random realizations of  $S_{\text{ob}}^{\text{RX}_k}[i]$  in (39). When  $\mathbf{W}_{\text{TX}}^{j-1} = \mathbf{0}$ ,  $Q_{\text{FC}}[j]$  for SA-ML can be obtained by replacing  $\geq$ ,  $<$ , and  $\xi_{\text{FC}}^{\text{ad}, \text{SA}}[j]$  with  $>$ ,  $=$ , and 0 in (39), respectively.

## V. NUMERICAL RESULTS AND SIMULATIONS

In this section, we present numerical and simulation results to examine the error performance of the different ML detection variants. We simulate using a particle-based method considered in [33], where the precise locations of all individual molecules are known. Since we model the RXs and the FC as passive observers, in our simulation all molecules persist indefinitely once they are released. Unless otherwise noted, we consider the environmental parameters in Table II. In the following figures, we vary  $t_{\text{trans}}$  (which also changes  $\Delta t_{\text{RX}}$  and  $T$ ),  $M_{\text{FC}}$  (which also changes  $\Delta t_{\text{FC}}$ ), and  $K$ . Since the topology is symmetric, we consider the same decision threshold at all RXs such that  $\xi_{\text{RX}_k} = \xi_{\text{RX}}$ ,  $\forall k$ .

In the following, we assume that the TX releases  $S_0 = 10000$  molecules for symbol “1” and the total number of molecules released by all RXs for symbol “1” is fixed at 2000. Thus for MD-ML and SD-ML, each RX releases  $S_{\text{D}} = \lfloor 2000/K \rfloor$  molecules to report a decision of “1”. For SA-ML, each RX uses the amplification factor  $\alpha = 157$ , such that the number of molecules released by all RXs for transmission of one symbol, averaged over all considered sequences of 20 symbols, is 1000. We consider a system that consists of at most six RXs. The specific locations of the TX, RXs, and FC are listed in Table III. Furthermore, the simulated error probabilities are averaged over independent transmissions of 50000 randomly-generated TX symbol sequences.

In order to provide trade-offs between the performance versus the information available, we compare the error performance of the proposed ML detection variants with that of existing alternatives, i.e., the majority rule considered in [13], [14], SD-Constant considered in [15], and (simple) soft fusion in [13]. In simple soft fusion<sup>5</sup>, the FC makes a decision  $\hat{W}_{\text{FC}}[j]$  by comparing the sum  $s_j^{\text{RX}}$  with  $\xi_{\text{FC}}$ . It can be shown that  $Q_{\text{FC}}[j]$  for simple soft fusion with *any* realization of  $\mathbf{W}_{\text{TX}}^{j-1}$  can be obtained by replacing  $\xi_{\text{FC}}^{\text{ad}}[j]$  with the constant  $\xi_{\text{FC}}$  in (23). We also propose one additional variant for comparison, namely, SA-Constant. In SA-Constant, the behavior of each RX is the same as that in SA-ML, but the FC makes a decision  $\hat{W}_{\text{FC}}[j]$  by comparing  $s_j^{\text{FC}}$  with a constant threshold  $\xi_{\text{FC}}$ , independent of  $\mathbf{W}_{\text{TX}}^{j-1}$ . It can be shown that  $Q_{\text{FC}}[j]$  for SA-Constant with *any* realization of  $\mathbf{W}_{\text{TX}}^{j-1}$  can be obtained by replacing  $\xi_{\text{FC}}^{\text{ad,SA}}[j]$  with the threshold  $\xi_{\text{FC}}$  in (39). We summarize all perfect and noisy reporting variants considered in this section in Table IV and Table V, respectively. For these variants, we consider the same parameters as for the ML detection variants listed in Table II and described above. This ensures that the fairness of our comparisons.

In the following figures, we clarify that the value of  $\bar{Q}_{\text{FC}}^*$  is the minimum  $\bar{Q}_{\text{FC}}$  by numerically optimizing the corresponding constant decision thresholds of each considered variant. Unless otherwise noted, we emphasize that these thresholds are constants that are optimized once over all realizations of  $\mathbf{W}_{\text{TX}}^{j-1}$  and all symbol intervals.

In the following figures, for each ML detection variant, we plot the error probability with the local history and genie-aided history. We observe that for all ML detection variants, the error performance using the local history has a very small degradation from that using the genie-aided history. This demonstrates the effectiveness of our proposed method to estimate the symbols previously transmitted by the TX (and by all the RXs for SD-ML and MD-ML). We also observe that the simulations have very strong agreement with the analytical results, thereby validating our analytical results, especially L-ML, SD-ML, and SA-ML with the genie-aided history.

In Fig. 2, we consider the perfect reporting scenario. We plot the optimal average global error probability versus the transmission time interval for F-ML, L-ML, the majority rule, and the soft fusion variant. For each  $t_{\text{trans}}$ , we keep  $M_{\text{RX}}$  and  $t_{\text{report}}$  fixed as in Table II, and let  $\Delta t_{\text{RX}}$  and  $T$  be  $\Delta t_{\text{RX}} = t_{\text{trans}}/2M_{\text{RX}}$  and  $T = t_{\text{trans}} + t_{\text{report}}$ , respectively. In other words, except for  $\Delta t_{\text{RX}}$ ,  $t_{\text{trans}}$ , and  $T$ , all other parameters remain fixed. We first observe that F-ML and L-ML achieve a significant error performance improvement over the majority rule and the soft fusion variant. This demonstrates the advantage of ML detection for the cooperative MC system, even though the ML detection is applied on a symbol-by-symbol basis. Second, we observe that for the majority rule, the error performance gain for the soft fusion variant is minimal relative to that achieved with ML detection. This observation is not surprising since the decision rule of L-ML is comparing the sum of all RXs' observations with the *adaptive* threshold  $\xi_{\text{FC}}^{\text{ad}}[j]$ , while the soft

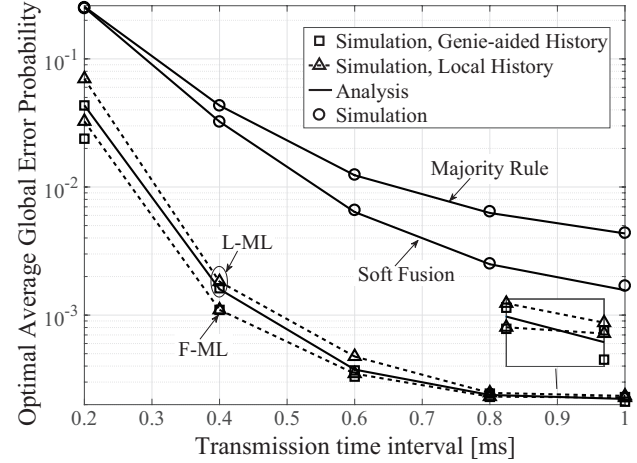


Fig. 2. Optimal Average global error probability  $\bar{Q}_{\text{FC}}^*$  of different variants versus the transmission time interval  $t_{\text{trans}}$  with  $K = 3$  in the perfect reporting scenario. The analytical error performance of the majority rule is presented in [14].

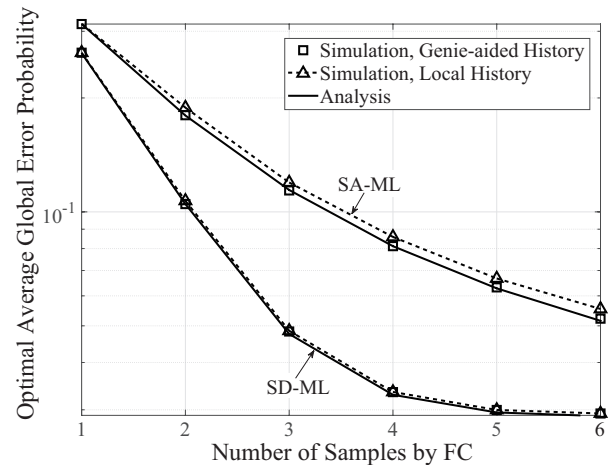


Fig. 3. Optimal average global error probability  $\bar{Q}_{\text{FC}}^*$  of the SD-ML and SA-ML variants versus the number of samples by FC  $M_{\text{FC}}$  with  $K = 1$  in the noisy reporting scenario.

fusion variant compares this sum with a *constant* threshold  $\xi_{\text{FC}}$ . Third, we observe that F-ML outperforms L-ML. This is due to the fact that the likelihood of every sample by each RX is considered separately in F-ML, whereas only the sum of all samples by each RX are considered in L-ML. Finally, we see that the system error performance improves as  $t_{\text{trans}}$  increases. This is because when  $t_{\text{trans}}$  and  $T$  increase, the ISI decreases.

In Figs. 3–4, we consider the noisy reporting scenario. We plot the optimal average global error probability  $\bar{Q}_{\text{FC}}^*$  of different variants versus the number of samples by the FC  $M_{\text{FC}}$ . In Figs. 3–4, the report time interval is fixed at  $t_{\text{report}} = 0.3$  ms as in Table II and the time step at the FC for each  $M_{\text{FC}}$  is  $\Delta t_{\text{FC}} = 0.3$  ms/ $M_{\text{FC}}$ .

In Fig. 3, we consider a single-RX system (which is analogous to the two-hop environment considered in [31]). We plot the optimal average global error probability of the SD-ML and SA-ML variants versus the number of samples by the FC. We first observe that the error performance degradation using the local history compared to the genie-aided history

<sup>5</sup>We introduced and tested simple soft fusion in [13], but we did not analyze its error performance in [13].

TABLE IV  
SUMMARY OF CONSIDERED PERFECT REPORTING VARIANTS

Variants	Available Information at FC	Behavior at FC
L-ML	Individual sample at each RX: $s_{j,m}^{\text{RX}_k}$	Assess joint likelihood of samples $s_{j,m}^{\text{RX}_k}$
F-ML	Sum of samples at each RX: $s_j^{\text{RX}_k}$	Assess joint likelihood of sums $s_j^{\text{RX}_k}$
Soft Fusion [13]	Sum of samples at all RXs: $s_j^{\text{RX}}$	Compare $s_j^{\text{RX}}$ with constant $\xi_{\text{FC}}$
Majority Rule [13], [14]	Binary decision of each RX: $\hat{W}_{\text{RX}_k}[j]$	Combine decisions $\hat{W}_{\text{RX}_k}[j]$

TABLE V  
SUMMARY OF CONSIDERED NOISY REPORTING VARIANTS

Variants	Relaying at RXs	Molecules Used in All RXs	Behavior at FC
Majority Rule [13], [14]	DF	Multiple-type	Combine estimated decisions
MD-ML	DF	Multiple-type	Assess joint likelihood of $K$ sums $s_{j,k}^{\text{FC}}$
SD-Constant [15]	DF	Single-type	Compare $s_j^{\text{FC}}$ with constant $\xi_{\text{FC}}$
SD-ML	DF	Single-type	Assess likelihood of $s_j^{\text{FC}}$
SA-Constant	AF	Single-type	Compare $s_j^{\text{FC}}$ with constant $\xi_{\text{FC}}$
SA-ML	AF	Single-type	Assess likelihood of $s_j^{\text{FC}}$

for SD-ML is much smaller than that for SA-ML. This is because in SD-ML, previous RX symbols can be accurately estimated by the FC using ML detection from the RX-FC links. However, for SA-ML, the FC does not directly estimate the previous RX emissions from the RX-FC links and the FC just generates many possible previous RX emissions based on estimated TX symbols, hence the error in the estimation of previous TX symbols propagates to the estimated previous RX emissions. Second, we observe that SD-ML outperforms SA-ML. This is because in SA-ML,  $\text{RX}_k$  amplifies the ISI at  $\text{RX}_k$  in the current symbol interval due to the previous TX symbols. However, we note that SD-ML requires more computational processing at the RXs since they need to decode the TX's symbols, whereas SA-ML is more biologically realistic. Finally, we observe that the system error performance improves as  $M_{\text{FC}}$  increases. This is because when  $M_{\text{FC}}$  increases, the number of molecules expected to be observed at each RX increases.

In Fig. 4, we consider a three-RX system. We plot the optimal average global error probability versus the number of samples by the FC for MD-ML and the majority rule, SD-ML and SD-Constant, and SA-ML and SA-Constant in Figs. 4(a), 4(b), and 4(c), respectively. We first observe that the degradation with the local history for SA-ML is more noticeable than that for MD-ML and SD-ML. In fact, we made a similar observation in Fig. 3 and it can be explained with similar reasons, i.e., in SA-ML, the FC does not estimate the previous emissions of the RXs in the same way as SD-ML. Second, we observe that MD-ML, SD-ML, and SA-ML outperform the majority rule, SD-Constant, and SA-Constant, respectively, i.e., MD-ML, SD-ML, and SA-ML provide lower bounds on the error probability for the majority rule, SD-Constant, and SA-Constant, respectively. Specifically, the error performance degradation with these simpler cooperative variants are all within an order of magnitude for the range of  $M_{\text{FC}}$  considered. This demonstrates the relatively good performance of the simpler cooperative variants. We emphasize that these simpler cooperative variants are more realistic to implement in the MC domain.

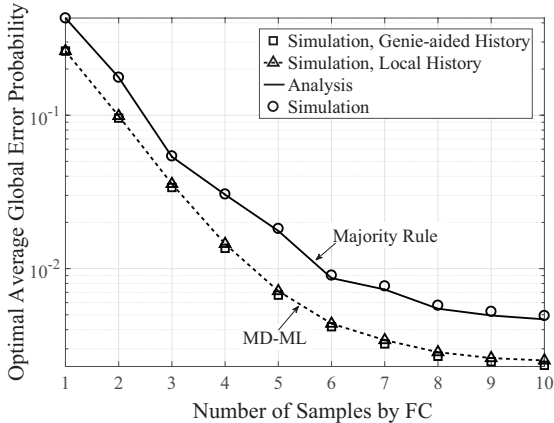
In Fig. 5, we plot the optimal average global error probability versus the number of cooperative RXs for SD-ML, SA-ML, SD-Constant, and SA-Constant in the noisy reporting scenario.

The observations for SD-ML and SD-Constant are consistent with our observations in Fig. 4(b) and the observations for SA-ML and SA-Constant are consistent with our observations in Fig. 4(c). We also observe that SD-Constant outperforms SA-ML using the local history except when  $K = 4$  and  $K = 5$ , which demonstrates the good performance of SD-Constant relative to SA-ML. Moreover, we see that the system error performance improves as  $K$  increases, even though the total number of molecules used in the cooperative MC system is constrained.

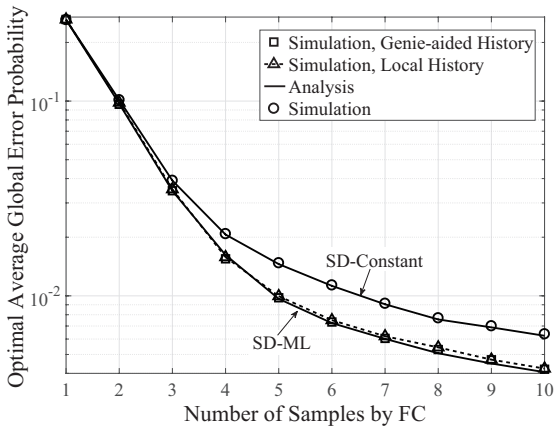
In Fig. 6, we plot the optimal average global error probability versus the number of cooperative RXs for MD-ML, SD-ML, SA-ML, and the majority rule in the noisy reporting scenario, and L-ML in the perfect reporting scenario. The observations for MD-ML and the majority rule are consistent with our observations in Fig. 4(a). Otherwise, we first observe that the error performance reduction with the majority rule, compared to SD-ML, is within an order of magnitude for the range of  $K$  considered. Second, we observe that the majority rule outperforms SA-ML using the local history. These observations demonstrate the good performance of the majority rule, relative to SD-ML and SA-ML. Third, we observe that L-ML has a significant error performance improvement over MD-ML and the majority rule, i.e., L-ML provides a lower bound on the achievable error performance of the system in the noisy reporting scenario. Fourth, we observe that MD-ML outperforms SD-ML and SD-ML outperforms SA-ML. This is because the knowledge of individual  $s_{j,k}^{\text{FC}}$  for each  $\text{RX}_k - \text{FC}$  link in MD-ML improves detection performance over only knowing the sum  $s_j^{\text{FC}}$  in SD-ML. Comparing to  $\text{RX}_k$  making binary decision in the current symbol interval in SD-ML,  $\text{RX}_k$  amplifies the ISI at  $\text{RX}_k$  in the current symbol interval due to the previous TX symbols in SA-ML. In addition, we see again that the system error performance improves as  $K$  increases, even with a limit on the total number of molecules.

## VI. CONCLUSIONS

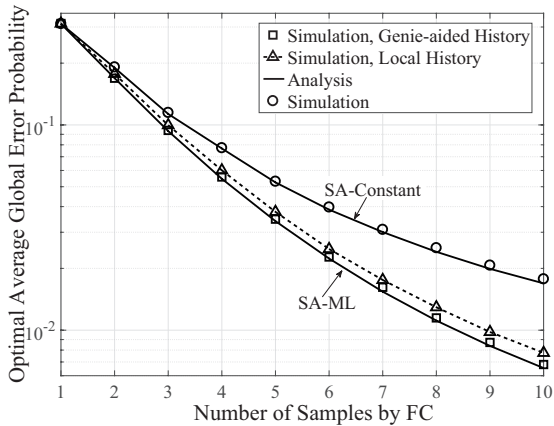
Combined with our initial work in [25], we presented for the first time symbol-by-symbol ML detection for the cooperative diffusion-based MC system with multiple communication phases. This approach enables us to determine lower bounds



(a) MD-ML and the majority rule



(b) SD-ML and SD-Constant



(c) SA-ML and SA-Constant

Fig. 4. Optimal average global error probability  $\bar{Q}_{FC}^*$  versus the number of samples by FC  $M_{FC}$  with  $K = 3$  in the noisy reporting scenario for (a) MD-ML and the majority rule, (b) SD-ML and SD-Constant, and (c) SA-ML and SA-Constant. The analytical error performance of the majority rule and SD-Constant is presented in [14] and [15], respectively.

on the error performance of simpler cooperative variants. We considered the transmission of a sequence of binary symbols and accounted for the resultant ISI in the design and analysis of the cooperative MC system. We presented five ML detection variants with different constraints on the knowledge available at the FC, i.e., F-ML, L-ML, MD-ML, SD-ML, and SA-ML.

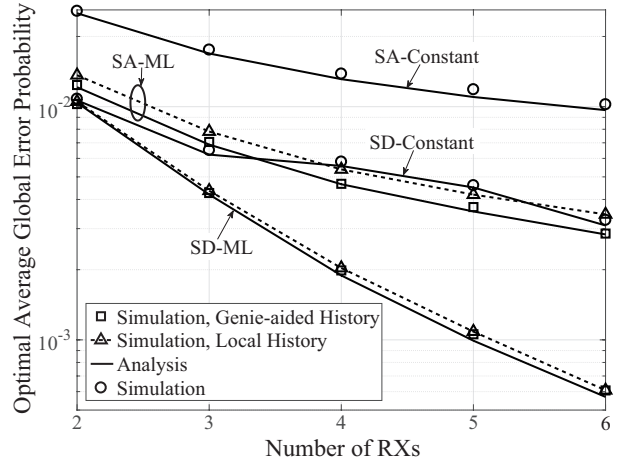


Fig. 5. Optimal average global error probability  $\bar{Q}_{FC}^*$  of different variants versus the number of RXs  $K$  in the noisy reporting scenario. The analytical error performance of SD-Constant is presented in [15].

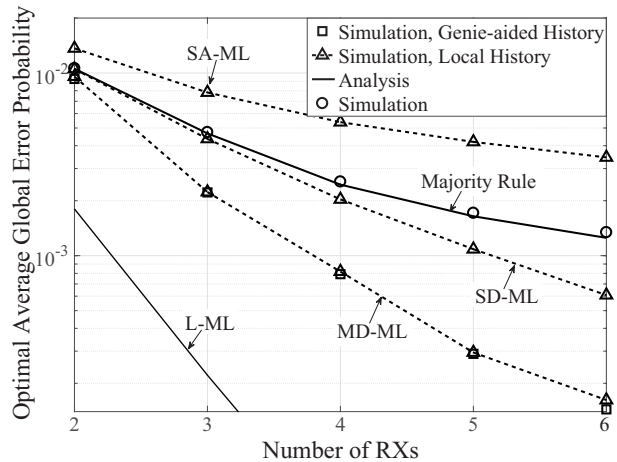


Fig. 6. Optimal average global error probability  $\bar{Q}_{FC}^*$  of different variants versus the number of RXs  $K$  in the noisy reporting scenario. The analytical error performance of the majority rule is presented in [14].

For practicality, the FC chooses the current symbol using its own local history. For tractability, we derived the system error probabilities for L-ML, SD-ML, and SA-ML using the genie-aided history. The analytical expressions for system error probabilities for L-ML and SA-ML are given in closed form. Using numerical and simulation results, we corroborated the accuracy of these analytical expressions. We demonstrated the good performance of the simpler cooperative variants in [13]–[15] relative to the noisy reporting variants of ML detectors, e.g., the error performance degradation with these simpler cooperative variants, compared to noisy ML detector variants, are all within an order of magnitude in Section V. Our results revealed the trade-off among the performance, knowledge of previously-transmitted symbols, the types of molecule available, and computational complexity.

## APPENDIX

### PROOF OF THEOREM 2

We first prove the decision rule for SD-ML when  $\hat{\lambda}_N^D[j] > 0$ . To this end, based on (5), we first rewrite the general decision rule for SD-ML as  $\hat{W}_{FC}[j] = 1$  if  $\frac{\mathcal{L}_1^{SD}[j]}{\mathcal{L}_0^{SD}[j]} \geq 1$ , otherwise  $\hat{W}_{FC}[j] = 0$ . Thus, if  $\frac{\mathcal{L}_1^{SD}[j]}{\mathcal{L}_0^{SD}[j]}$  is a monotonically increasing function with respect to  $s_j^{FC}$ , then we can obtain the decision rule above. To prove  $\frac{\mathcal{L}_1^{SD}[j]}{\mathcal{L}_0^{SD}[j]}$  is a monotonically increasing function with respect to  $s_j^{FC}$ , we take the first derivative of  $\frac{\mathcal{L}_1^{SD}[j]}{\mathcal{L}_0^{SD}[j]}$  with respect to  $s_j^{FC}$  as

$$\begin{aligned} & \frac{\partial \mathcal{L}_1^{SD}[j]}{\partial s_j^{FC}} \mathcal{L}_0^{SD}[j] - \frac{\partial \mathcal{L}_0^{SD}[j]}{\partial s_j^{FC}} \mathcal{L}_1^{SD}[j] \\ &= \left( \sum_{Z=0}^K \sum_{Z_1=0, Z>Z_1}^K \binom{K}{Z} \binom{K}{Z_1} \right. \\ & \quad \times \exp \left( -2\hat{\lambda}_N^D[j] - Z\hat{\lambda}_s^D[j] - Z_1\hat{\lambda}_s^D[j] \right) AB \\ & \quad \times \left( \hat{\lambda}_N^D[j] + Z\hat{\lambda}_s^D[j] \right)^{s_j^{FC}} \left( \hat{\lambda}_N^D[j] + Z_1\hat{\lambda}_s^D[j] \right)^{s_j^{FC}} \\ & \quad \times \left( \mathcal{L}_0^{SD}[j] (s_j^{FC}!) \right)^{-2}, \end{aligned} \quad (40)$$

where

$$A = \log \left( \left( \hat{\lambda}_N^D[j] + Z\hat{\lambda}_s^D[j] \right) / \left( \hat{\lambda}_N^D[j] + Z_1\hat{\lambda}_s^D[j] \right) \right) \quad (41)$$

and

$$\begin{aligned} B &= (1 - P_{md}[j])^Z P_{md}[j]^{K-Z} P_{fa}[j]^{Z_1} \\ & \quad \times (1 - P_{fa}[j])^{K-Z_1} - (1 - P_{md}[j])^{Z_1} P_{md}[j]^{K-Z_1} \\ & \quad \times P_{fa}[j]^Z (1 - P_{fa}[j])^{K-Z}. \end{aligned} \quad (42)$$

In (40), we note that in each summand, except for  $AB$ , all terms are positive. Here, we have  $A \geq 0$  since  $Z \geq Z_1$  for the inner sum. We note that  $B \geq 0$  if  $1 - P_{md}[j] - P_{fa}[j] \geq 0$  holds and  $Z > Z_1$ . In fact, the condition  $1 - P_{md}[j] - P_{fa}[j] \geq 0$  is always valid. Thus, we have  $AB \geq 0$  and (40) is always non-negative. This proves that  $\frac{\mathcal{L}_1^{SD}[j]}{\mathcal{L}_0^{SD}[j]}$  is a monotonically increasing function with respect to  $s_j^{FC}$ . Thus, we obtain the decision rule when  $\hat{\lambda}_N^D[j] > 0$ . The decision rule when  $\hat{\lambda}_N^D[j] = 0$  can be proven analogously to the proof of Theorem 1. This completes the proof.

## REFERENCES

- [1] W. Guo, T. Asyhari, N. Farsad, H. B. Yilmaz, B. Li, A. W. Eckford, and C.-B. Chae, "Molecular communications: Channel model and physical layer techniques," *IEEE Trans. Wireless Commun.*, vol. 23, no. 4, pp. 120–127, Aug. 2016.
- [2] T. Nakano, A. W. Eckford, and T. Haraguchi, *Molecular Communication*. Cambridge, UK: Cambridge University Press, 2013.
- [3] T. Nakano and J. Q. Liu, "Design and analysis of molecular relay channels: An information theoretic approach," *IEEE Trans. Nanobiosci.*, vol. 9, no. 3, pp. 213–221, Sep. 2010.
- [4] S. M. Baylor and S. Hollingworth, "Calcium indicators and calcium signalling in skeletal muscle fibres during excitation-contraction coupling," *Prog. Biophys. Mol. Biol.*, vol. 105, pp. 162–179, June 2010.
- [5] B. Atakan and O. B. Akan, "On molecular multiple-access, broadcast, and relay channels in nanonetworks," in *Proc. ICST BIONETICS*, Nov. 2008, pp. 16:1–16:8.
- [6] M. J. Moore, T. Suda, and K. Oiwa, "Molecular communication: Modeling noise effects on information rate," *IEEE Trans. Nanobiosci.*, vol. 8, no. 2, pp. 169–180, June 2009.
- [7] T. Nakano, Y. Okaie, and A. V. Vasilakos, "Transmission rate control for molecular communication among biological nanomachines," *IEEE J. Sel. Areas Commun.*, vol. 31, no. 12, pp. 835–846, Dec. 2013.
- [8] C. T. Chou, "Extended master equation models for molecular communication networks," *IEEE Trans. Nanobiosci.*, vol. 12, no. 2, pp. 79–92, June 2013.
- [9] A. Einolghozati, M. Sardari, and F. Fekri, "Design and analysis of wireless communication systems using diffusion-based molecular communication among bacteria," *IEEE Trans. Wireless Commun.*, vol. 12, no. 12, pp. 6096–6105, Dec. 2013.
- [10] —, "Networks of bacteria colonies: A new framework for reliable molecular communication networking," *Nano Commun. Networks*, vol. 7, pp. 17–26, 2016.
- [11] B. H. Koo, C. Lee, H. B. Yilmaz, N. Farsad, A. W. Eckford, and C.-B. Chae, "Molecular MIMO: From theory to prototype," *IEEE J. Sel. Areas Commun.*, vol. 34, no. 3, pp. 600–614, Mar. 2016.
- [12] T. Furubayashi, T. Nakano, A. W. Eckford, and T. Yomo, "Reliable end-to-end molecular communication with packet replication and retransmission," in *Proc. IEEE GLOBECOM*, Dec. 2015, pp. 1–6.
- [13] Y. Fang, A. Noel, N. Yang, A. W. Eckford, and R. A. Kennedy, "Distributed cooperative detection for multi-receiver molecular communication," in *Proc. IEEE GLOBECOM*, Dec. 2016, pp. 1–7.
- [14] —, "Convex optimization of distributed cooperative detection in multi-receiver molecular communication," submitted to *IEEE Trans. Mol. Bio. Multi-Scale Commun.*, pp. 1–16, 2016. [Online]. Available: arXiv:1611.05590
- [15] Y. Fang, A. Noel, Y. Wang, and N. Yang, "Simplified cooperative detection for multi-receiver molecular communication," in *Proc. IEEE ITW*, Nov. 2017, pp. 1–5.
- [16] J. G. Proakis, *Digital Communication*, 4th ed. New York: McGraw-Hill, 2000.
- [17] D. Kilinc and O. B. Akan, "Receiver design for molecular communication," *IEEE J. Sel. Areas Commun.*, vol. 31, no. 12, pp. 705–714, Dec. 2013.
- [18] A. Noel, K. C. Cheung, and R. Schober, "Optimal receiver design for diffusive molecular communication with flow and additive noise," *IEEE Trans. Nanobiosci.*, vol. 13, no. 3, pp. 350–362, Sept. 2014.
- [19] L. S. Meng, P. C. Yeh, K. C. Chen, and I. F. Akyildiz, "On receiver design for diffusion-based molecular communication," *IEEE Trans. Signal Process.*, vol. 62, no. 22, pp. 6032–6044, Nov. 2014.
- [20] M. U. Mahfuz, D. Makrakis, and H. T. Mouftah, "A comprehensive analysis of strength-based optimum signal detection in concentration-encoded molecular communication with spike transmission," *IEEE Trans. Nanobiosci.*, vol. 14, no. 1, pp. 67–83, Jan. 2015.
- [21] A. Singhal, R. K. Mallik, and B. Lall, "Performance analysis of amplitude modulation schemes for diffusion-based molecular communication," *IEEE Trans. Wireless Commun.*, vol. 14, no. 10, pp. 5681–5691, Oct. 2015.
- [22] T. C. Mai, M. Egan, T. Q. Duong, and M. D. Renzo, "Event detection in molecular communication networks with anomalous diffusion," *IEEE Commun. Lett.*, vol. 21, no. 6, pp. 1249–1252, June 2017.
- [23] R. Mosayebi, V. Jamali, N. Ghoroghchian, R. Schober, M. N. Kenari, and M. Mehrabi, "Cooperative abnormality detection via diffusive molecular communications," pp. 1–30. [Online]. Available: arXiv:1703.10084
- [24] U. Rogers and M. S. Koh, "Parallel molecular distributed detection with brownian motion," *IEEE Trans. Nanobiosci.*, vol. 15, no. 8, pp. 871–880, Dec. 2016.
- [25] Y. Fang, A. Noel, N. Yang, A. W. Eckford, and R. A. Kennedy, "Maximum likelihood detection for cooperative molecular communication," 2017, pp. 1–7, submitted to *IEEE ICC 2018*. [Online]. Available: arXiv:1704.05623
- [26] J. Suzuki, D. H. Phan, and H. Budiman, "A nonparametric stochastic optimizer for TDMA-based neuronal signaling," *IEEE Trans. Nanobiosci.*, vol. 13, no. 3, pp. 244–254, Sept. 2014.
- [27] A. Ahmadzadeh, A. Noel, A. Burkowski, and R. Schober, "Amplify-and-forward relaying in two-hop diffusion-based molecular communication networks," in *Proc. IEEE GLOBECOM*, Dec. 2015, pp. 1–7.
- [28] M. S. Kuran, H. B. Yilmaz, T. Tugeu, and I. F. Akyildiz, "Modulation techniques for communication via diffusion in nanonetworks," in *Proc. IEEE ICC*, June 2011, pp. 1–5.
- [29] H. ShahMohammadian, G. G. Messier, and S. Magierowski, "Blind synchronization in diffusion-based molecular communication channels," *IEEE Commun. Lett.*, vol. 17, no. 11, pp. 2156–2159, Nov. 2013.

- [30] S. Abadal and I. F. Akyildiz, "Bio-inspired synchronization for nanocommunication networks," in *Proc. IEEE GLOBECOM*, Dec. 2011, pp. 1–5.
- [31] A. Ahmadzadeh, A. Noel, and R. Schober, "Analysis and design of multi-hop diffusion-based molecular communication networks," *IEEE Trans. Mol. Biol. Multi-Scale Commun.*, vol. 1, no. 2, pp. 144–157, June 2015.
- [32] A. Noel, K. C. Cheung, and R. Schober, "Using dimensional analysis to assess scalability and accuracy in molecular communication," in *Proc. IEEE ICC*, June 2013, pp. 818–823.
- [33] S. S. Andrews and D. Bray, "Stochastic simulation of chemical reactions with spatial resolution and single molecule detail," *Physical Biology*, vol. 1, no. 3, pp. 135–151, Aug. 2004.